Electronic Supplementary Information

Binding Affinities of Cucurbit[*n*]urils with Cations

Shuai Zhang, [‡a] Laura Grimm, [‡b] Zsombor Miskolczy, [c] László Biczók, [c]
Frank Biedermann *[b] Werner M. Nau *[a]

[a] Department of Life Sciences and Chemistry, Jacobs University Bremen, Campus Ring 1, 28759 Bremen, Germany

[b] Institute of Nanotechnology, Karlsruhe Institute of Technology (KIT), Hermann-von-Helmholtz Platz 1, 76344 Eggenstein-Leopoldshafen, Germany

[c] Institute of Materials and Environmental Chemistry, Research Centre for Natural Sciences, P.O. Box 286, 1519 Budapest, Hungary

[‡] These authors contributed equally.

Table of Contents

1. Literature Survey of Binding Constants of CB*n* with Cations

Several authors have previously studied the binding of inorganic cations with individual CB*n*, which are compiled in Table S1. Mock and co-workers already reported the first binding constant of NH_4^+ with CB6 in 1986, $\log(K_a/M^{-1}) = 1.92$, at 40 °C in a 1:1 H_2O/formic acid mixture.[1] In the following decades, Buschmann and co-workers contributed significantly to the investigation of the binding constants between earth cations and CB6 as well as CB5;[2-7] the methods, which included UV-Vis and ITC titrations as well as TOC measurements (total organic carbon), afforded quite different values for the same cation. Recently, fluorescence competitive displacement titrations were used for obtaining the binding constants of CB7 to metal cations by Pischel in 2014.[8] p*K*a values of CB6 (3.02) and CB7 (2.2) were measured by Buschmann[2] in 1992 and Kim[9] in 2007 by absorption titration with HCl, respectively, and these values are entered as binding constants to hydronium in Table 1 in the main text and in Table S1.

Table S1: Logarithmic binding constants, $\log(K_a/M^{-1})$, for 1:1 complexation of inorganic cations with CB*n* (*n* = 5-8) in H_2O at ambient temperature (25 °C) unless stated differently.

Host	CB6[2]	CB6[3]	CB6[4]	CB6[4]	CB5[5, 6]	CB6[5, 6]	CB6[7]	CB7[8]
Method	UV	UV	ITC	ITC	TOC	TOC	ITC	UV/F
Year	1992	1994	1998	1998	2001	2001	2003	2014
Additive	---	52% HCO_2H	50% HCO_2H	---	---	---	50% HCO_2H	---
H_3O^+	3.02							
NH_4^+	3.97	2.23			1.32	2.84		
Li^+		2.23	2.38					1.41
Na^+	3.69	3.16	3.23	3.47	1.85	3.49		2.18
K^+	3.96	2.75	2.79		1.31	2.85		1.85
Rb^+	4.41	2.61	2.68		1.01	2.98		2.76
Cs^+	4.82				0.90	2.52		2.84
Ag^+								
Mg^{2+}								1.62
Ca^{2+}	4.57		2.80		1.73	3.61		3.15
Sr^{2+}			3.18		1.50	2.90		3.64
Ba^{2+}			2.83	5.23	1.32			
Zn^{2+}					1.45	2.22		2.34
Ni^{2+}					1.27	1.58		
Cu^{2+}					1.77	1.75		
Yb^{3+}							2.76	
La^{3+}							2.64	
Fe^{3+}					1.88	1.60		

2. Determination of Binding Constants

We found for the relatively well water-soluble CB5 homologue that ITC experiments produced sufficiently large binding heats when they were conducted at 283 K. In favourable cases, sigmoidal binding isotherms were observed see Figures S1-S19, which provided access to the binding stoichiometry. All observations, including control experiments at different concentration ratios (see Table S4-S6), were fully consistent with the formation of a 1:1 CB5•M^{m+} complex, where the potential subsequent binding of a second cation to the other carbonyl portal is at least a factor of 10 weaker, likely due to electrostatic repulsion. We therefore discuss in the main text the binding constants (K_a) for the 1:1 CB5•M^{m+} complexes.

For the larger CB*n* homologues ($n \geq 6$), we adopted the indicator displacement strategy to determine the binding affinities of cations. To minimize interferences from occasionally observed ternary CB*n*•dye•M^{m+} complexes for small fluorophores,[10-14] we selected three pH-independent and large indicator dyes, namely, trans-4-[4-(dimethylamino)styryl]-1-methylpyridinium iodide (DSMI) for CB6,[15, 16] berberine chloride (BE) for CB7,[17] and a perylene bis(diimide) derivative (PDI) for CB8[18, 19] (Scheme S1). Optical titration-based binding isotherms obtained for the displacement of BE from CB7 are shown in Section 6. For the relatively water-soluble host CB7, the binding affinity for La^{3+} could also be obtained at 283 K by ITC measurements to afford log K_a = 5.25 (at 298 K, the heats of binding were small), in good agreement with the value obtained through the indicator displacement approach at the same temperature, log K_a = 5.28.

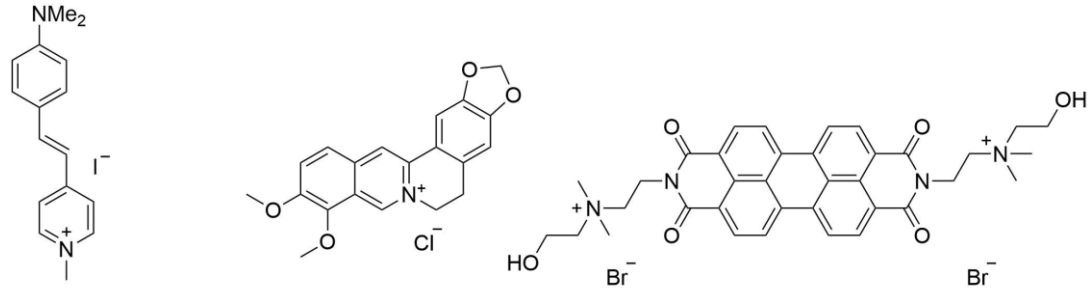

DSMI **berberine** **PDI**

Scheme S1: Chemical structures of the indicator dyes used for CB6, CB7, and CB8, respectively.

Fitting of the fluorescence and ITC data with a binding model that explicitly accounts for the binding of two metal cations to the CB*n* rims was also performed (see Fig. S1-S3 and Table S4-S6); the resulting affinities for the binding of the second cation equivalent were at least one order of magnitude lower than for the first binding step and associated with large

errors, such that the discussion in the main text focuses on the binding constants for formation of the 1:1 CB*n*•M^{m+} complexes.

As previously demonstrated for CX4,[20] the binding of hydronium ions can be incorrectly interpreted as a protonation of a cation-receptor host. To differentiate between the two different alternatives, one needs to compare the apparent binding constants for hydronium ion binding with the pK_a value of a comparable monomer; in the case of CB*n*, a sensible choice appears to be tetramethylurea, which has a pK_a of –0.14.[21] This value falls below the values determined for CB6 and CB7,[22] see Table 1 in main text, which supports the interpretation of the measured binding constant as a hydronium ion binding.[9] The dependence of the hydronium ion binding on the size of the macrocycle is also characteristic for the binding of a monovalent cation. It should be noted that for other cation receptors, such as Cryptand[2.2.2], a protonation of the acceptor can actually occur rather than hydronium ion binding (see Table 1 in main text).[23]

3. Error Estimation

The statistical errors from the titration fittings were generally not larger than 10% in the K_a values. The reproducibility error, that is, when the measurements were performed multiple times, was up to 20% and therefore larger. For example, when the binding constants of Ba^{2+} was determined by fitting of seven repeated fluorescence displacement titrations (3 μM BE, 0.5 μM CB7) with identical instrumental settings, the log K_a values were 5.22, 5.24, 5.38, 5.29, 5.28, 5.29, and 5.27, which corresponds to a measured log K_a of 5.28 ± 0.05. When repeating ITC titrations with CB5 at least three times, the errors were 15% in K_a and 1.0 kJ mol^{-1} in ΔH, ΔG and $-T\Delta S$. We conservatively estimate the errors of the reported values in Table 1 in the main text and in Tables S2 and S3 as being 0.10 in log K_a or 25% in K_a and ±1.0 kJ mol^{-1} for the thermochemical data.

4. Materials and Methods

All commercial chemicals used in this study were purchased from Sigma-Aldrich, Fluka, Strem Chemicals, and Newburyport and used without further purification; an exception was CB6, which was obtained from H.-J. Buschmann (Universität Duisburg-Essen, Germany). The "content" of the CB*n* samples was found to be between 78-80% by ITC titrations with berberine (for CB7) or by ^{1}H NMR measurements (using β-cyclodextrin), indicating 20-22% water or salt content. CB5 was additionally desalted with a Biotech Grade Dialysis Membrane (Cellulose Ester/Regenerated Cellulose) System, because the NH_4^+ content of the commercial sample was

found to significantly affect the ITC experiments (see Section 5.4). The CB5 concentration of the solution was determined by ITC titration experiments with $La(NO_3)_3$. The determined concentration value was in accordance with that determined by ITC titration experiments with other metal nitrates. The pH of the solutions was measured with a WTW 330I pH meter equipped with a combined pH glass electrode (SenTix Mic). A minimum amount of hydrochloric acid or sodium hydroxide solutions were used for adjusting the pH, since excessive Na^+ or H_3O^+ concentrations affect the complexation between CB*n* and guest molecules. The concentration of berberine and the metal nitrates in solution was accurately determined by using their molar absorption coefficients (berberine: 22500 $M^{-1}cm^{-1}$ at 344 nm and nitrate: 9500 M^{-1} cm^{-1} at 201 nm).[24-26] UV-Vis measurements were either done on a Varian Cary 4000 UV-Vis spectrophotometer or on a Jasco V-730 UV-Vis/NIR spectrophotometer.

5. ITC Experiments for CB5 and CB7

All ITC experiments for the CB5 complexes were carried out on a Microcal PEAQ-ITC from Malvern at 10 °C. To determine the thermodynamic parameters for CB5 the ITC data was analyzed by the Malvern instrument software with the one-set-of-sites model (for the concentration dependency study the sequential-binding model was also used, see below), and the first data point was always omitted. In a typical experiment with CB5, 3 µL metal nitrate solution (the first injection was 0.4 µL) with 150 seconds spacing and 5 µcal/second reference power were injected 13 times into the ITC cell (stir speed: 750 rpm; initial delay: 60 s; injection duration: 6 s), which contained the host at a ca. 10-15 times lower concentration. Unless states differently, the data were baseline-corrected by the average value of the titration curve of $M^{m+}(NO_3)_n$ (m = 1-3) into water. The Ba^{2+} concentration of Ba^{2+}-stock solutions decreased upon standing due to the formation of insoluble salts; the Ba^{2+} concentration was therefore adjusted by fixing the known CB5 concentration and forcing N (sides) to 1.

To determine the CB7 concentration by ITC, berberine (c_1 = 750 µM, c_2 = 500 µM) was added stepwise in a series of 19 injections (the first injection was 0.2 µL, then 2 µL each) at an interval of 150 seconds at 25 °C. The average dilution heat, which was determined by adding a berberine solution into water under the same conditions as in the titration of CB7, was subtracted. The ITC fitting equations are built into the Malvern analysis software. They can be found in the user manual from page 99 onwards: https://jeltsch.org/sites/jeltsch.org/files/files/MicroCal-PEAQ-ITC-Analysis-Software-User-Manual-English-MAN576-01-EN-00.pdf

5.1. Thermochemical Parameters for CB5 from ITC

Table S2: Thermochemical parameters (±1.0 kJ/mol error) characterizing the complexation of selected cations by CB5 at 10 °C in water. Averaged data from at least three repetition experiments. Experiments were corrected for heats of dilution.

Cation	ΔG / kJ mol^{-1}	ΔH / kJ mol^{-1}	$-T\Delta S$ / kJ mol^{-1}
NH_4^+	–14.1	–11.5	–2.5
Na^+	–21.4	–2.3	–19.0
K^+	–24.9	–12.5	–13.1
Rb^+	–17.5	–19.1	1.6
Cs^+	–14.0	–35.4	21.3
Ca^{2+}	–14.4	–12.8	–1.6
Sr^{2+}	–28.0	–7.9	–20.0
Ba^{2+}	–34.9	–19.6	–15.3
Yb^{3+}	–20.1	17.0	–37.1
La^{3+}	–22.7	24.5	–47.1

5.2. Thermochemical Parameters for CB7 from ITC

Table S3: Thermodynamic parameters (±1.0 kJ/mol error) characterizing the 1:1 complexation of cations by CB7 at 25 °C in water. Experiments were corrected for heats of dilution.

Cation	ΔG / kJ mol^{-1}	ΔH / kJ mol^{-1}	$-T\Delta S$ / kJ mol^{-1}
H_3O^+	–12.0	–6.4[a]	–5.6[a]
K^+	–18.8	–8.7	–10.1
Rb^+	–19.5	–9.9	–9.6
Cs^+	–20.0	–9.7	–10.3
Ca^{2+}	–22.9	–9.8	–13.1
Sr^{2+}	–24.6	–14.3	–10.3
Ba^{2+}	–27.2	–16.0	–11.2

. [a] Measurement was conducted at 10 °C

5.3. ITC Experiments to Test Different Data Fitting Models

1. $La(NO_3)_3$

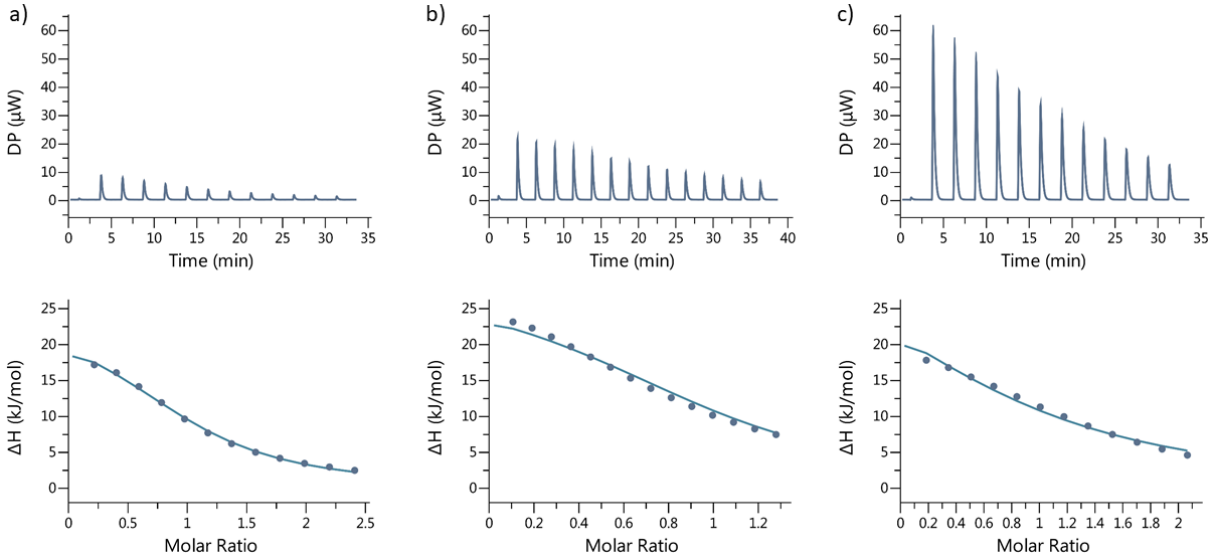

Figure S1: ITC isotherm (dilution corrected) for the titration of $La(NO_3)_3$ into aqueous CB5 solution at 10 °C. **a)** c($La(NO_3)_3$) = 2.50 mM and c(CB5) = 200 µM; **b)** c($La(NO_3)_3$) = 6.93 mM, and c(CB5) = 800 µM; **c)** c($La(NO_3)_3$) = 18.0 mM and c(CB5) = 1.68 mM. All fits show shown were performed with the one-set-of-sites model. Dilution heat correction was applied in all instances.

Table S4: Thermodynamic parameters characterizing the complexation of La^{3+} by CB5 at different concentrations in water. Comparison of data fitting with the one set of sites (OSS) model and sequential binding (SB) model. $K_{a,1}$ was fixed in the analysis with SB model to the value determined at the lowest CB5 and cation concentration (c(CB5) = 200 µM and c($La(NO_3)_3$) = 2.5 mM).

		c(CB5) / µM	c(Cation) / mM	K_a / 10^3 M^{-1}		log K_a		ΔH / kJ/mol		–TΔS / kJ/mol	
				1	2	1	2	1	2	1	2
a)	OSS	200	2.50	14.9 ± 0.09		4.17		24.5 ± 0.5		–47.1	
b)	OSS	800	6.93	4.66 ± 0.22		3.67		28.3 ± 1.3		–48.3	
	SB	800	6.93	**14.9**	3.66 ± 1.06	**4.17**	3.56	25.7 ± 0.2	–3.44 ± 0.9	–48.3	–15.9
c)	OSS	900	7.78	2.92 ± 0.56		3.46		33.9 ± 0.9		–52.7	
	SB	900	7.78	**14.9**	2.79 ± 4.0	**4.17**	3.45	25.6 ± 0.3	1.32 ± 1.5	–48.2	–20.0
d)	OSS	1680	18.0	0.59 ± 0.05		2.77		39.8 ± 0.5		–54.9	
	SB	1680	18.0	**14.9**	2.89 ± 4.0	**4.17**	3.46	18.20 ± 0.1	7.13 ± 0.3	–40.9	–25.9

In conclusion, the one-set-of-sites model fits the ITC data well at relatively low concentration of CB5 and $La(NO_3)_3$. Some deviations are found in the higher concentration range, which may justify applying a sequential binding model to fit the binding of a second metal cation to the second rim of CB5. However, other effects such as aggregation of CB5 at higher concentration may also explain the deviations. Be this as it may, that the binding affinity of the second cation, $K_{a,2}$, is at least one order of magnitude weaker than $K_{a,1}$.

2. $Sr(NO_3)_2$

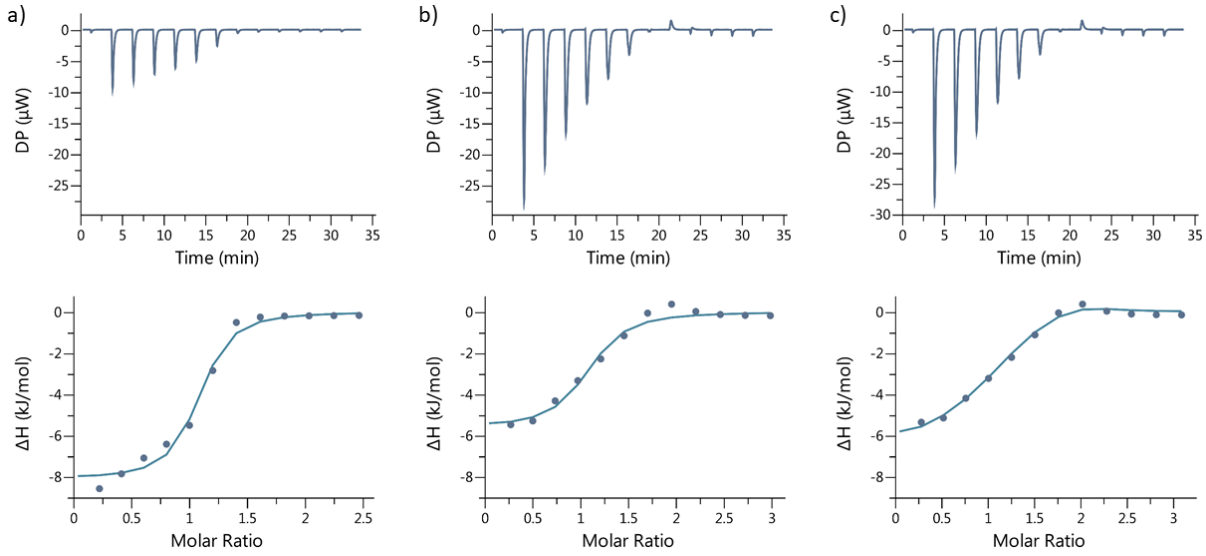

Figure S2: ITC isotherms for the titration of $Sr(NO_3)_2$ into aqueous CB5 solution at 10°C. **a)** c($Sr(NO_3)_2$) = 5.10 mM and c(CB5) = 400 µM **b)** c($Sr(NO_3)_2$) = 26.9 mM and c(CB5) = 1.68 mM, **c)** c($Sr(NO_3)_2$) = 26.9 mM and c(CB5) = 1.68 mM. For a) and b), fits were performed with the one-set-of-sites model. For c), the sequential-binding model was used. Dilution heat correction was applied in all instances.

Table S5: Thermodynamic parameters characterizing the complexation of Sr^{2+} by CB5 at different concentrations in water. Comparison of data fitting with the one set of sites (OSS) model and sequential binding (SB) model. $K_{a,1}$ was fixed in the analysis with SB model to the value determined at the lowest CB5 and cation concentration (c(CB5) = 400 µM and c($Sr(NO_3)_2$) = 5.1 mM).

		c(CB5) µM	/c(Cation) / mM	K_a / $\cdot 10^3$ M^{-1}		log K_a		ΔH / kJ/mol		-TΔS / kJ/mol	
				1	2	1	2	1	2	1	2
a)	OSS	400	5.1	143 ± 6.0		5.16		–7.9 ± 0.3		–20.0	
	OSS	1680	19.0	10.1 ± 1.9		4.00		–6.0 ± 0.3		–15.7	
	SB	1680	19.0	**143**	26.0 ± 1.2	**5.16**	4.42	-6.4 ± 0.1	1.1 ± 0.3	-21.6	-25.1
b)	OSS	1680	26.9	12.9 ± 2.6		4.11		-5.7 ± 0.3		-16.7	
	SB	1680	26.9	**143**	16.2 ± 1.4	**5.16**	4.21	-5.9 ± 0.1	0.7 ± 0.2	-22.1	-23.5
c)	OSS	1680	28.5	14.0 ± 2.4		4.15		-5.5 ± 0.3		-17.0	
	SB	1680	28.5	**143**	13.5 ± 7.2	**5.16**	4.13	-5.7 ± 0.2	0.6 ± 0.2	-22.3	-23.0

In conclusion, the one-set-of-sites model fits the ITC data well at relatively low concentration of CB5 and $Sr(NO_3)_2$. Some deviations are found in the higher concentration range, which may justify applying a sequential binding model to fit the binding of a second metal cation to the second rim of CB5. However, other effects such as aggregation of CB5 at higher concentration may also explain the deviations. Be this as it may, that the binding affinity of the second cation, $K_{a,2}$, is at least one order of magnitude weaker than $K_{a,1}$.

3. KNO_3

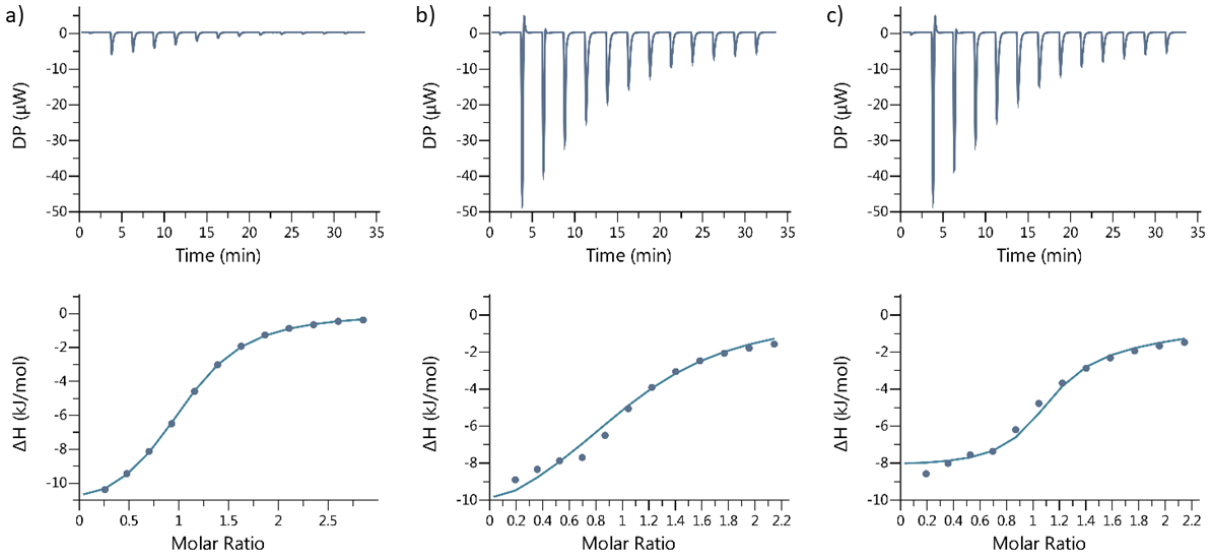

Figure S3: Comparison of the determined values in dependence on concentration. ITC isotherms for the titration of KNO_3 into aqueous CB5 solution at 10 °C. **a)** c(KNO_3) = 2.70 mM and c(CB5) = 174 µM, **b)** c(KNO_3) = 18.5 mM and c(CB5) = 1.68 mM, **c)** c(KNO_3) = 18.5 mM and c(CB5) = 1.68 mM. For a) and b), fits were performed with the one-set-of-sites model. For c), the sequential-binding model was used. Dilution heat correction was applied in all instances.

Table S6: Thermodynamic parameters characterizing the complexation of K^+ by CB5 at different concentrations in water. Comparison of data fitting with the one set of sites (OSS) model and sequential binding (SB) model. $K_{a,1}$ was fixed in the analysis with SB model to the value determined at the lowest CB5 and cation concentration (c(CB5) = 174 µM and c(KNO_3) = 2.70 mM).

		c(CB5) / µM	c(Cation) /	K_a /·10^3 M^{-1}		log K_a		ΔH / kJ/mol		–TΔS / kJ/mol	
				1	2	1	2	1	2	1	2
a)	OSS	174	2.70	53.3 ± 0.03		4.73		–12.5 ± 0.4		–13.1	
b)	OSS	1680	18.5	2.19 ± 0.12		3.34		–12.4 ± 0.7		–5.7	
	SB	1680	18.5	**53.3**	2.60 ± 0.15	**4.73**	3.41	–8.6 ± 0.3	–2.3 ± 0.2	–16.9	–16.0

In conclusion, the one-set-of-sites model fits the ITC data well at relatively low concentration of CB5 and KNO_3. Some deviations are found in the higher concentration range, which may justify applying a sequential binding model to fit the binding of a second metal cation to the second rim of CB5. However, other effects such as aggregation of CB5 at higher concentration may also explain the deviations. Be this as it may, that the binding affinity of the second cation, $K_{a,2}$, is at least one order of magnitude weaker than $K_{a,1}$.

5.4. ITC Experiments Comparing Commercial CB5 and Desalted CB5

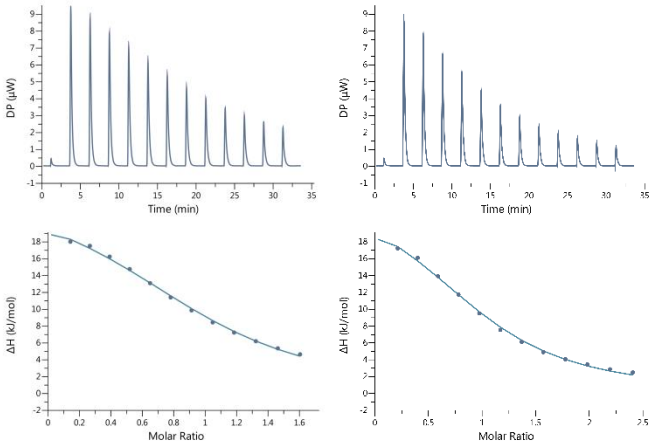

Figure S4: ITC isotherms for the titration of $La(NO_3)_3$ (2.5 mM) into a solution of CB5 (left, commercially available, 300 µM; right, desalted, 200 µM) in aqueous solution at 10°C. Fits were performed with the one-set-of-sites model. Dilution heat correction was applied.

Table S7: Thermodynamic parameters characterizing the 1:1 complexation of La^{3+} by commercial, salt-containing CB5 and desalted CB5 in water.

Sample	K_a/ (10^3 M^{-1})	log (K_a/M^{-1})	ΔG / (kJ/mol)	ΔH / (kJ/mol)	$-T\Delta S$ / (kJ/mol)
commercial	12.0	4.08	–22.1	24.1	–46.2
desalted	14.9	4.17	–22.7	24.5	–47.1

Comparing the ITC results for commercial CB5 (which contains $(NH_4)_2SO_4$ salts from synthesis/separation steps) with desalinated CB5 (through dialysis with a regenerated cellulose membrane, 500 g/mol cut-off) yields clear indication that the presence of NH_4-salt contaminations yield apparent, lower affinities of CB5 to cations on account of competitive binding of NH_4^+. All CB5 experiments reported in this work were therefore conducted with desalinated CB5 samples.

5.5. ITC Graphs for CB5 and Cations

1) HNO_3

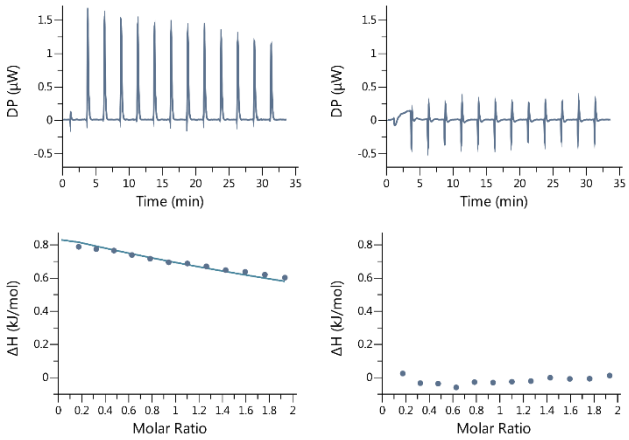

Figure S5: ITC isotherm (dilution corrected) for the titration of HNO_3 (c = 7.50 mM) into aqueous CB5 solution (left, c = 748 µM) and in water (right, average used for dilution heat correction) at 10 °C.

2) NH_4NO_3

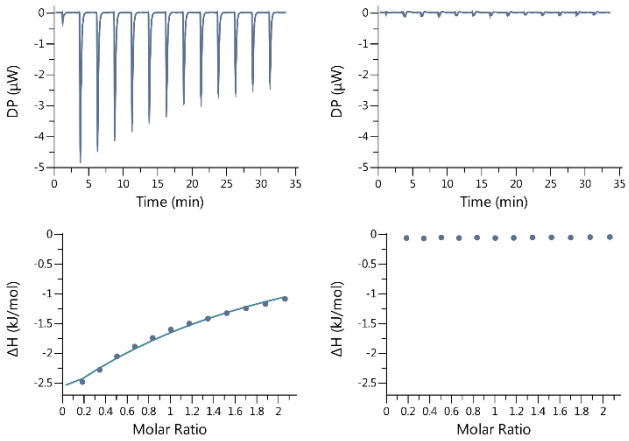

Figure S6: ITC isotherm (dilution corrected) for the titration of NH_4NO_3 (c = 8.00 mM) into aqueous CB5 solution (left, c = 748 µM) and in water (right, average used for dilution heat correction) at 10 °C.

3) $LiNO_3$

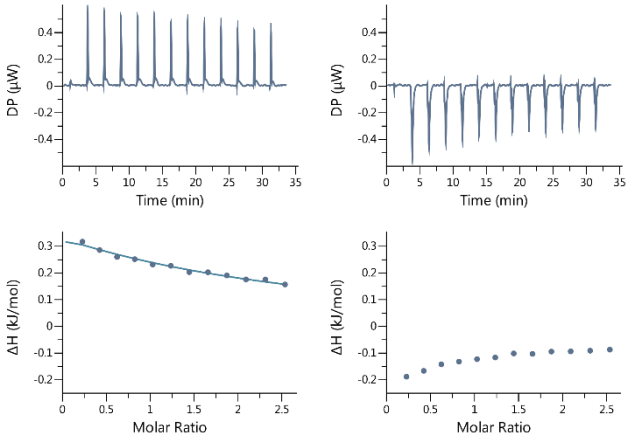

Figure S7: ITC isotherm (dilution corrected) for the titration of $LiNO_3$ (c = 15.0 mM) into aqueous CB5 solution (left, c = 1.14 mM) and in water (right, used for point-to-point correction) at 10 °C.

4) $NaNO_3$

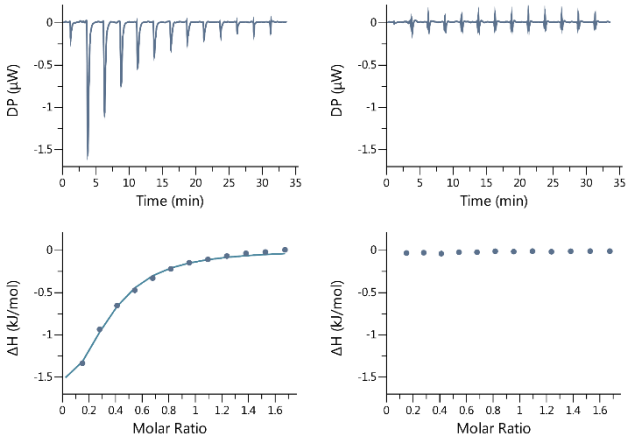

Figure S8: ITC isotherm (dilution corrected) for the titration of $NaNO_3$ (c = 6.50 mM) into aqueous CB5 solution (left, c = 748 µM) and in water (right, averaged value was used for dilution heat correction) at 10 °C.

5) KNO_3

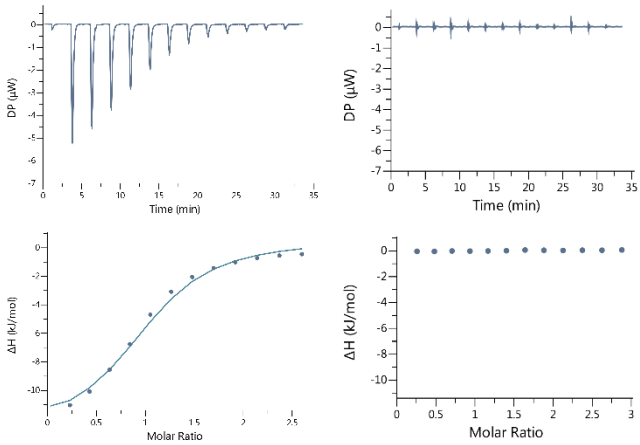

Figure S9: ITC isotherm (dilution corrected) for the titration of KNO_3 (c = 2.70 mM) into aqueous CB5 solution (left, c = 200 µM) and in water (right, average used for dilution heat correction) at 10 °C.

6) $RbNO_3$

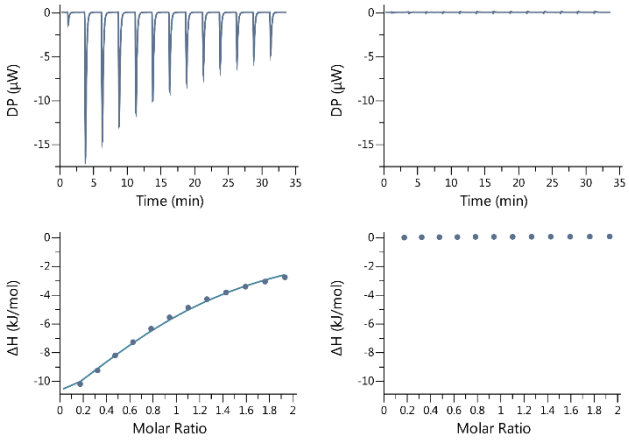

Figure S10: ITC isotherm (dilution corrected) for the titration of $RbNO_3$ (c = 7.50 mM) into aqueous CB5 solution (left, c = 748 µM) and in water (right, average used for dilution heat correction) at 10 °C.

7) $CsNO_3$

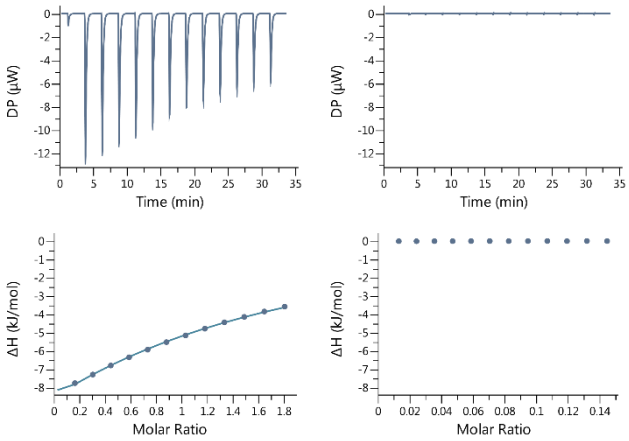

Figure S11: ITC isotherm (dilution corrected) for the titration of $CsNO_3$ (c = 7.00 mM) into aqueous CB5 solution (left, c = 748 µM) and in water (right, average used for dilution heat correction) at 10 °C.

8) $Mg(NO_3)_2$

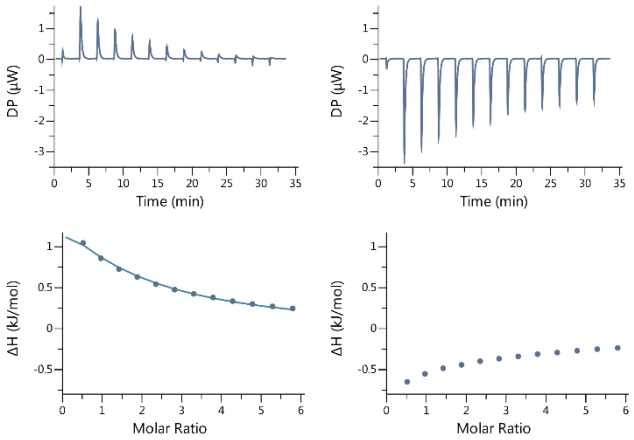

Figure S12: ITC isotherm (dilution corrected) for the titration of $Mg(NO_3)_2$ (c = 22.5 mM) into aqueous CB5 solution (left, c = 748 µM) and in water (right, used for point-to-point correction) at 10 °C.

9) $Ca(NO_3)_2$

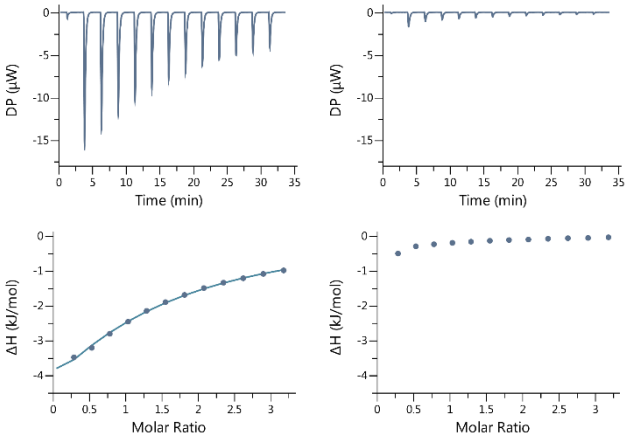

Figure S13: ITC isotherm (dilution corrected) for the titration of $Ca(NO_3)_2$ (c = 18.8 mM) into aqueous CB5 solution (left, c = 1.14 mM) and in water (right, used for point-to-point correction) at 10 °C.

10) $Sr(NO_3)_2$

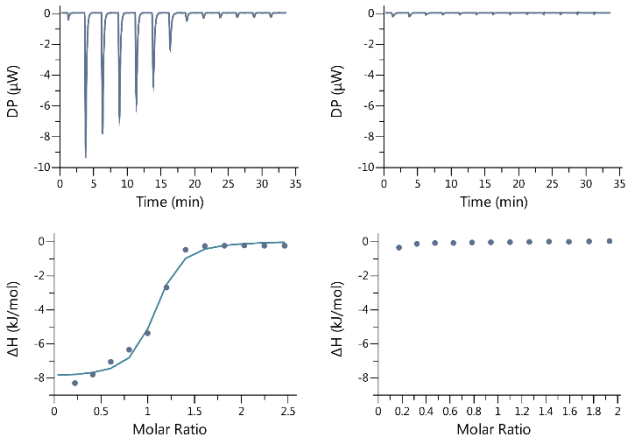

Figure S14: ITC isotherm (dilution corrected) for the titration of $Sr(NO_3)_2$ (c = 5.10 mM) into aqueous CB5 solution (left, c = 400 µM) and in water (right, average used for dilution heat correction) at 10 °C.

11) $Ba(NO_3)_2$

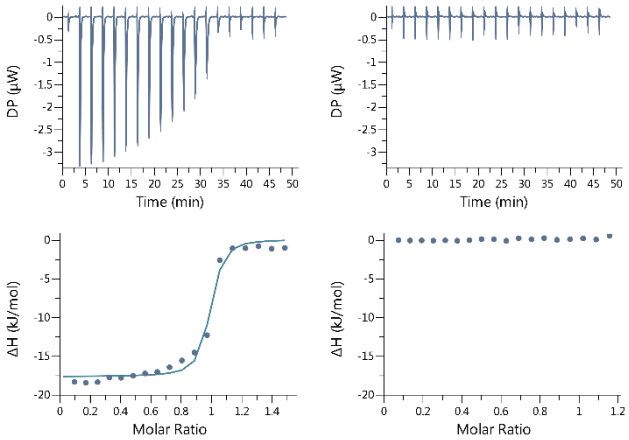

Figure S15: ITC isotherm (dilution corrected) for the titration of $Ba(NO_3)_2$ (c = 855 µM) into aqueous CB5 solution (left, c = 125 µM) and in water (right, average used for dilution heat correction) at 10 °C.

12) $Ni(NO_3)_2$

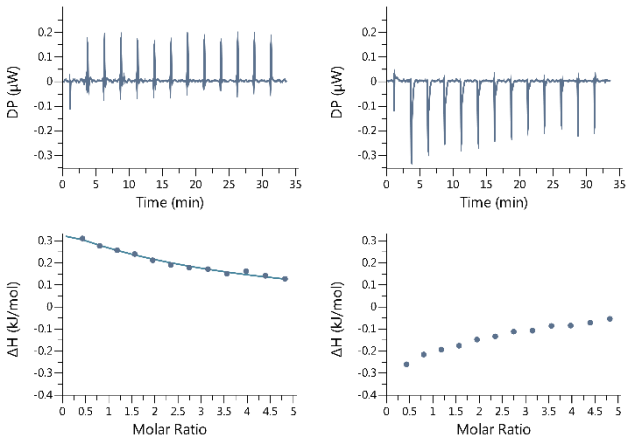

Figure S16: ITC isotherm (dilution corrected) for the titration of $Ni(NO_3)_2$ (c = 5 mM) into aqueous CB5 solution (left, c = 200 µM) and in water (right, average used for dilution heat correction) at 10 °C.

13) $Yb(NO_3)_3$

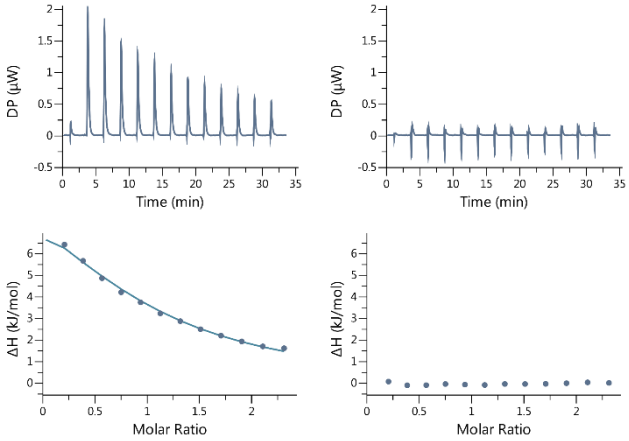

Figure S17: ITC isotherm (dilution corrected) for the titration of $Yb(NO_3)_3$ (c = 1.50 mM) into aqueous CB5 solution (left, c = 125 µM) and in water (right, average used for dilution heat correction) at 10 °C.

14) $La(NO_3)_3$

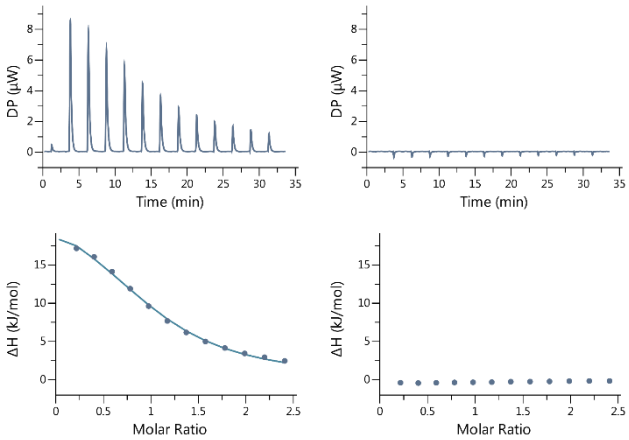

Figure S18: ITC isotherm (dilution corrected) for the titration of $La(NO_3)_3$ (c = 2.50 mM) into aqueous CB5 solution (left, c = 200 µM) and in water (right, used for point-to-point correction) at 10 °C.

15) $Fe(NO_3)_3$

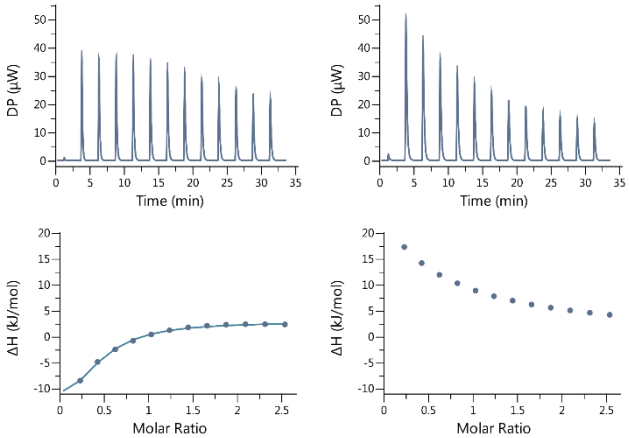

Figure S19: ITC isotherm (dilution corrected) for the titration of $Fe(NO_3)_3$ (c = 15.0 mM) into aqueous CB5 solution (left, c = 1.14 mM) and in water (right, used for point-to-point correction) at 10 °C. It was neither possible to fit the graph with N(sites) equals 1 nor to fit the graph without an extra offset (additional to the dilution heat subtraction).

5.6. ITC Graphs for CB7 and Cations

1) HNO_3

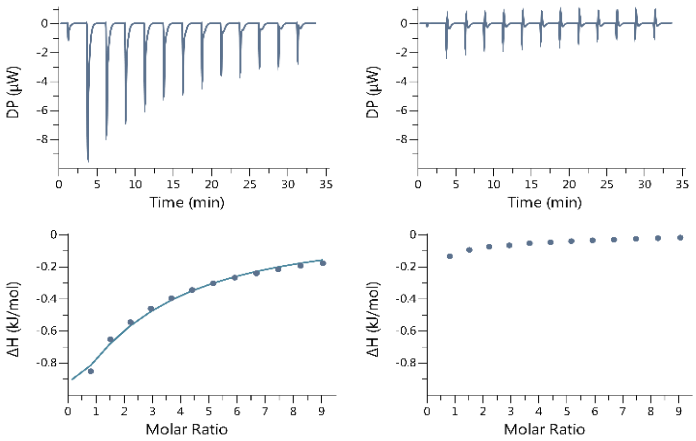

Figure S20: ITC isotherm for the titration of HNO_3 (c = 47.0 mM) into an aqueous CB7 solution (left, 1.00 mM) and in water (right, used for point-to-point correction) at 10 °C.

2) KCl

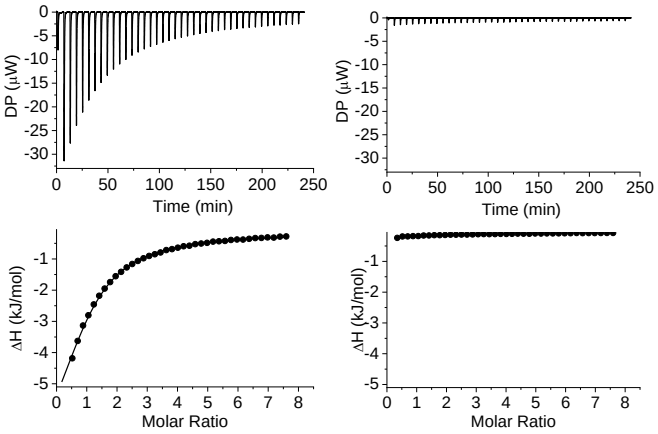

Figure S21: ITC isotherm (dilution corrected) for the titration of KCl (c = 27.0 mM) into aqueous CB7 solution (left, c = 0.761 mM) and into water (right, used for point-to-point correction) at 25 °C.

3) RbCl

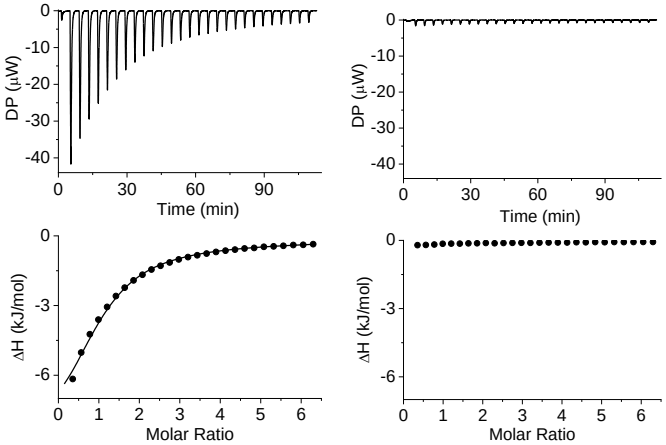

Figure S22: ITC isotherm (dilution corrected) for the titration of RbCl (c = 22.4 mM) into aqueous CB7 solution (left, c = 0.752 mM) and into water (right, used for point-to-point correction) at 25 °C.

4) CsCl

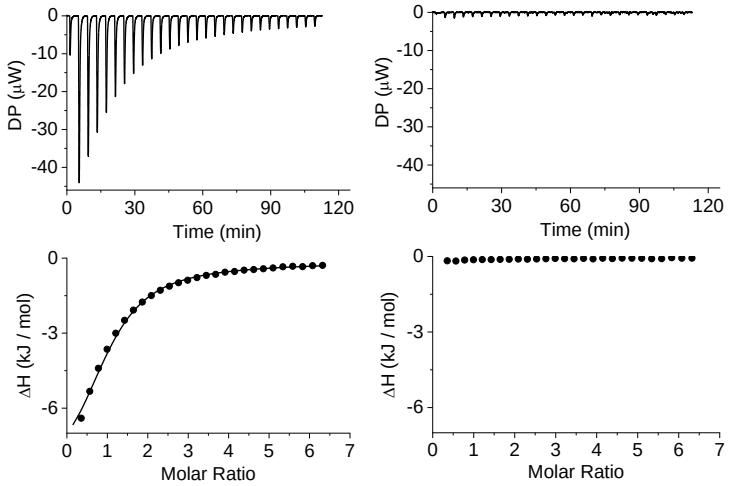

Figure S23: ITC isotherm (dilution corrected) for the titration of CsCl (c = 22.3 mM) into aqueous CB7 solution (left, c = 0.749 mM) and into water (right, used for point-to-point correction) at 25 °C.

5) $CaCl_2$

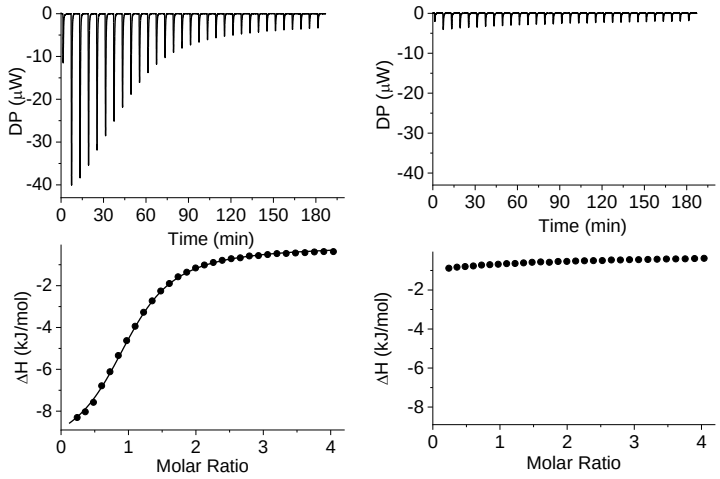

Figure S24: ITC isotherm (dilution corrected) for the titration of $CaCl_2$ (c = 14.4 mM) into aqueous CB7 solution (left, c = 0.761 mM) and into water (right, used for point-to-point correction) at 25 °C.

6) $SrCl_2$

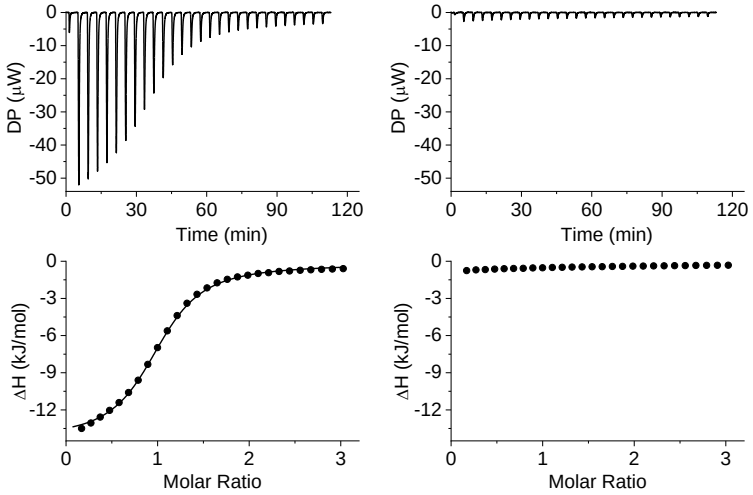

Figure S25: ITC isotherm (dilution corrected) for the titration of $SrCl_2$ (c = 10.7 mM) into aqueous CB7 solution (left, c = 0.747 mM) and into water (right, used for point-to-point correction) at 25 °C.

7) $BaCl_2$

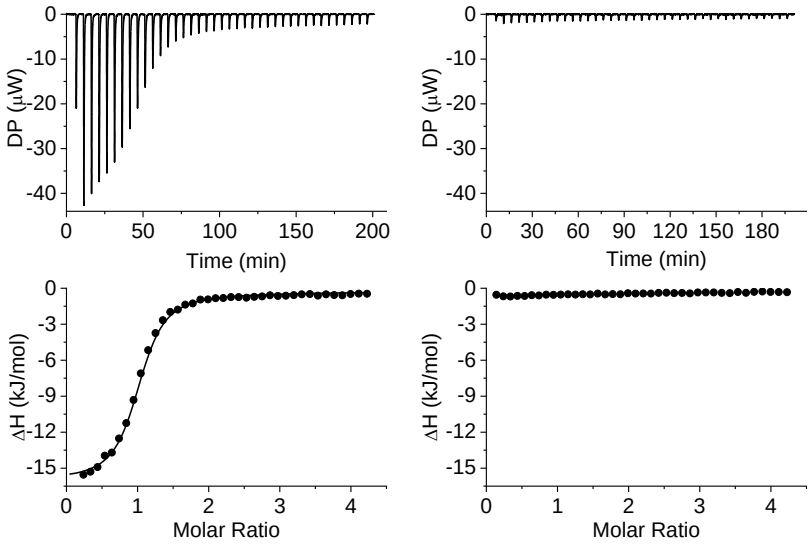

Figure S26: ITC isotherm (dilution corrected) for the titration of $BaCl_2$ (c = 10.1 mM) into aqueous CB7 solution (left, c = 0.505 mM) and into water (right, used for point-to-point correction) at 25 °C.

6. Dye Displacement Titrations for CB6, CB7, and CB8

UV-Vis measurements were either done on a Varian Cary 4000 UV-Vis spectrophotometer or on a Jasco V-730 UV-Vis/NIR spectrophotometer and fluorescence measurements were performed on a Varian Cary Eclipse Fluorimeter. All spectral experiments were conducted under air at ambient temperature in Millipore-grade H_2O. In the course of the optical titrations, all concentrations were kept constant except for that of the titrant. If not stated otherwise, binding constants were determined by using a 1:1 complexation model.

The binding constants for the selected cations with CB*n* (*n* = 6-8) were determined by using a competitive displacement model with Origin, section "Fitting Equations" below.

6.1. Fitting Equations for Analysis of Dye Displacement Titrations

The data obtained from the dye displacement titrations were fitted by two different competitive binding models and the derivation of the fitting equations is described here. For a simple stoichiometric displacement model, which assumes only the formation of 1:1 complexes between the indicator as well as the competitor (metal ion) and the host (Scheme S2), the relevant equilibrium constants are defined by eqs 1 and 2, where K_G is the association constant of the guest (fluorescence dye) with the host and K_C is the association constant of the competitor. [H], [G], [HC], and [HG] are the concentrations of the individual species.

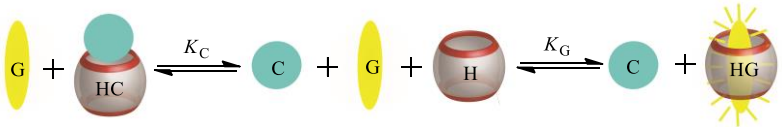

Scheme S2: Stoichiometric displacement model.

$$K_G = \frac{[HG]}{[H][G]} \quad (1)$$

$$K_C = \frac{[HC]}{[H][C]} \quad (2)$$

According to the law of mass conservation the concentrations can be expressed as follows, where G_0 is the total guest concentration (fluorescence dye) and H_0 is the total host concentration:

$$[G] = [G]_0 - [HG] \quad (3)$$

$$[C] = [C]_0 - [HC] \quad (4)$$

$$[H] = [H]_0 - [HC] - [HG] \quad (5)$$

From (1) follows with (3):

$$[HG] = \frac{K_G[H][G]_0}{1 + K_G[H]} \tag{6}$$

From (2) follows with (4):

$$[HC] = \frac{K_C[H][C]_0}{1 + K_C[H]} \tag{7}$$

From (5) with (6) and (7):

$$[H] = [H]_0 - \frac{K_C[H][C]_0}{1 + K_C[H]} - \frac{K_G[H][G]_0}{1 + K_G[H]} \tag{8}$$

The following equation can be derived from (8):

$$\begin{aligned} &K_C K_G[H]^3 + \\ &(K_C + K_G + K_C K_G[G]_0 + K_C K_G[C]_0 - K_C K_G[H]_0)[H]^2 + \\ &(K_C[C]_0 - K_C[H]_0 + K_G[G]_0 - K_G[H]_0 + 1)[H] \\ &-[H]_0 = 0 \end{aligned} \tag{9}$$

Substitution with:

$$a = K_C K_G$$

$$b = K_C + K_G + K_C K_G[G]_0 + K_C K_G[C]_0 - K_C K_G[H]_0$$

$$c = K_C[C]_0 - K_C[H]_0 + K_G[G]_0 - K_G[H]_0 + 1$$

$$d = -[H]_0$$

yields the following type of cubic equation:

$$a[H]^3 + b[H]^2 + c[H] + d = 0 \tag{10}$$

The conversion into fluorescence intensity is carried by using the molar fractions, where I_g is the fluorescence intensity of an uncomplexed guest (fluorescence dye) and I_{gh} is the fluorescence intensity of the host-guest complex:

$$FI = \frac{[G]}{[G]_0} I_g - \frac{[HG]}{[G]_0} I_{gh} \tag{11}$$

Substituted with (3) and (6), this simplifies to eq. 12:

$$FI = I_g + (I_{gh} - I_g)\ \frac{K_G[H]}{1+K_G[H]} \tag{12}$$

Eq. 12 can be implemented into commercial fitting programs by calling sub-routines for the solution of the cubic eq. 10. Since G_0, K_G, H_0, and I_g are known, the other unknown parameters ($K_C = K_a$ and I_{gh}) can be obtained through a nonlinear fitting procedure.

The alternative displacement model, see Scheme S3, assumes the formation of the same complexes as in the first model, but considers additionally the formation of a 2:1 competitor-

host complex to represent the docking of a second cation to the vacant portal. This requires the consideration of an additional equilibrium constant for this 2:1 complex, K_{CC}, and an additional species concentration, [HCC], while all other parameters are kept the same as for the derivation of the stoichiometric binding model, see eqs. 1-3.

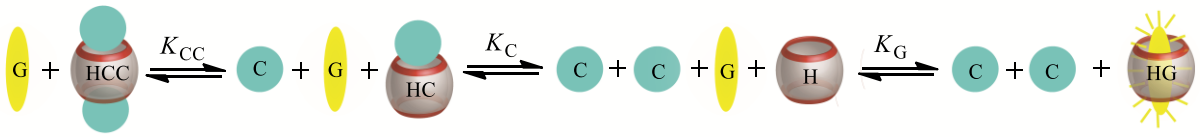

Scheme S3: Displacement model with the additional consideration of a 2:1 competitor-host complex.

Thus, the following equations can be derived:

$$K_G = \frac{[HG]}{[H][G]} \tag{13}$$

$$K_C = \frac{[HC]}{[H][C]} \tag{14}$$

$$K_{CC} = \frac{[HCC]}{[HC][C]} \tag{15}$$

According to law of mass conservation and the additional assumption of $[C]$ equals to $[C]_0$ (large excess of inorganic cations) one obtains:

$$[G] = [G]_0 - [HG] \tag{16}$$

$$[C] \approx [C]_0 \tag{17}$$

$$[H] = [H]_0 - [HC] - [HCC] - [HG] \tag{18}$$

The assumption that $[C]$ equals $[C]_0$ is fully justified when the large millimolar concentrations of added metal ions are contrasted to the micromolar concentrations of host and dye. From (13) follows with (16):

$$[HG] = \frac{K_G[H][G]_0}{1+K_G[H]} \tag{19}$$

From (14) follows with (17):

$$[HC] = K_C[H][C]_0 \tag{20}$$

From (15) follows with (17):

$$[HCC] = K_{CC}K_C[H][C]_0^2 \tag{21}$$

Substituting (19), (20), and (21) into (18) affords:

$$[H] = [H]_0 - K_C[H][C]_0 - K_{CC}K_C[H][C]_0^2 - \frac{K_G[H][G]_0}{1+K_G[H]} \tag{22}$$

The following equation can be derived from (22):

$$(K_G + K_C K_G[C]_0 + K_{CC} K_C K_G[C]_0^2)[H]^2 +$$
$$(1 - K_G[H]_0 + K_C[C]_0 + K_{CC} K_C[C]_0^2 + K_G[G]_0)[H]$$
$$-[H]_0 = 0 \quad (23)$$

Substitution with:

$$a = K_G + K_C K_G[C]_0 + K_{CC} K_C K_G[C]_0^2$$
$$b = 1 - K_G[H]_0 + K_C[C]_0 + K_{CC} K_C[C]_0^2 + K_G[G]_0$$
$$c = -[H]_0$$

yields a quadratic equation of the type:

$$a[H]^2 + b[H] + c = 0 \quad (24)$$

Eq. 12 can again be implemented into commercial fitting programs by now solving the quadratic eq. 12, and since G_0, K_G, H_0, and I_g are again known, the other unknown parameters (K_C = K_a, K_{CC}, and I_{gh}) can be obtained through a nonlinear fitting procedure, and the obtained K_C values can be compared with those obtained for the fitting according to model 1. An example of two fits of the same set of experimental data according to model 2 and 1 is shown in Fig. S2; as can be seen, the consideration of the 2:1 complex in model 2 does not have a strong effect on the 1:1 cation-host binding constants; we discuss the latter in the main text.

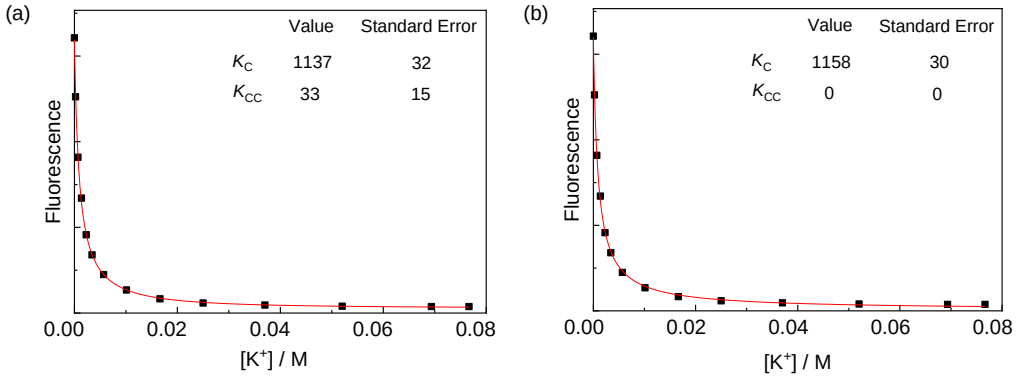

Figure S27: (a) Fitting of a set of displacement titration data according to model 2. (b) Fitting of the same set of displacement titration data according to model 1.

6.2. Potential Effect of Different Anions

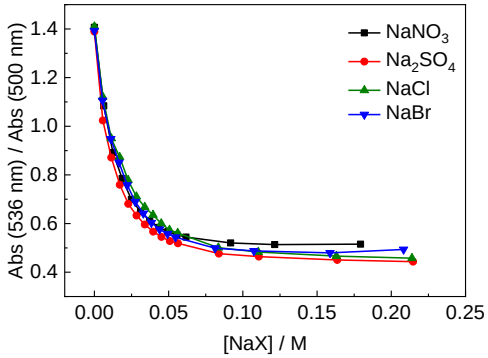

Figure S28: Plots of Abs (536 nm)/Abs (500 nm) of 15 µM PDI and 15 µM CB8 *versus* concentrations of four types of sodium salts (data points connected by lines, not fitted)

Conclusion: The minor dependence of the binding isotherm on the counter anion, if any, falls far below the much larger variations observed with cation type.

6.3. Competitive Displacement Experiments with CB6/DSMI and Cations

6.3.1. Determination of Binding Constant between CB6 and DSMI

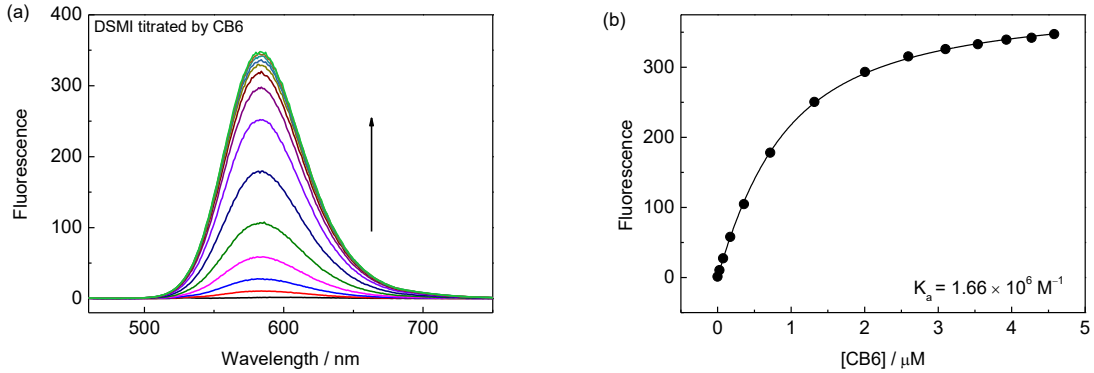

Figure S29: (a) Emission spectra of 0.5 µM DSMI, in aqueous solution, upon addition of CB6, λ_{ex} = 450 nm; (b) Plot of the emission intensity at 580 nm of 0.5 µM DSMI versus concentration of CB6.

6.3.2. Representative Displacement Titration of CB6/DSMI with K^+

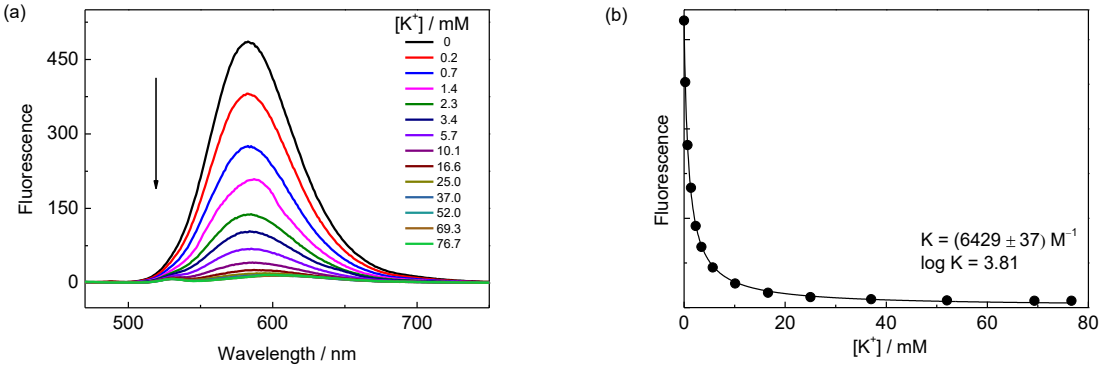

Figure S30: (a) Emission spectra of 3 µM DSMI and 0.5 µM CB6 in aqueous solution, upon addition of KCl, λ_{ex} = 450 nm; (b) Fitting plot of the emission intensity at 580 versus concentration of KCl.

6.3.3. Normalized Emission Intensity of CB6/DSMI *versus* Cation Concentration

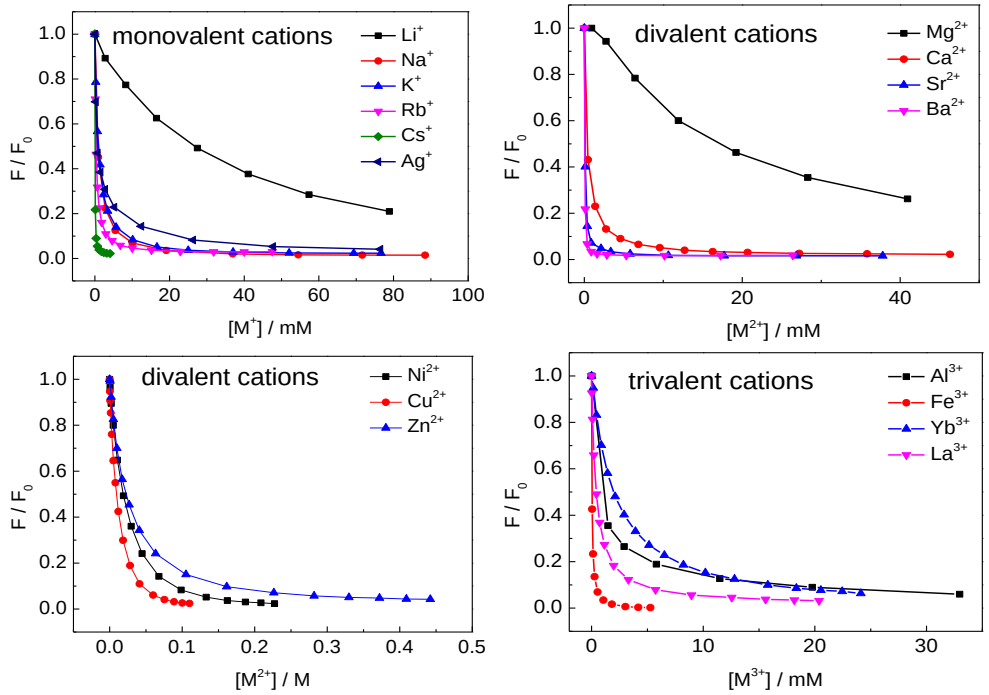

Figure S31: Plot of the normalized emission intensity at 580 nm of 3 µM DSMI and 0.5 µM CB6 versus concentrations of 17 different metal cations. (Data points connected by lines, not fitted.)

6.3.4. Fitting Curves of Displacement Titrations between CB6/DSMI and Cations

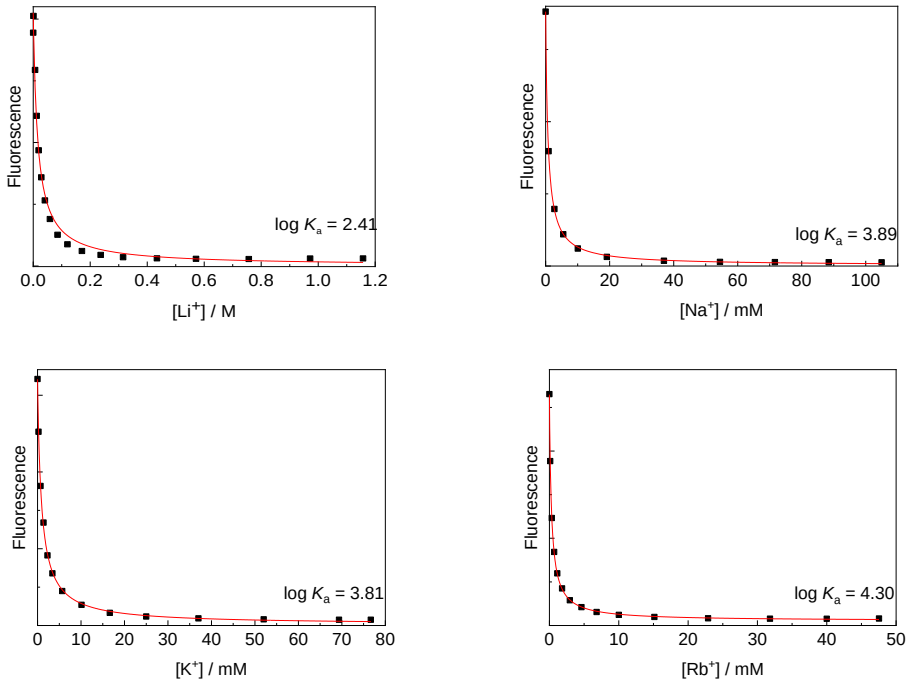

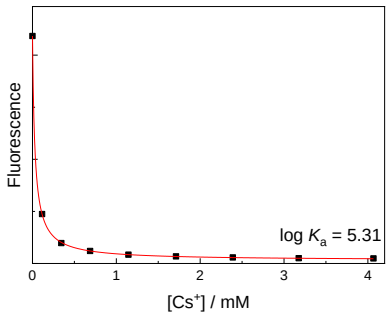
Fluorescence
log K_a = 5.31
0
1
2
3
4
[Cs^+] / mM

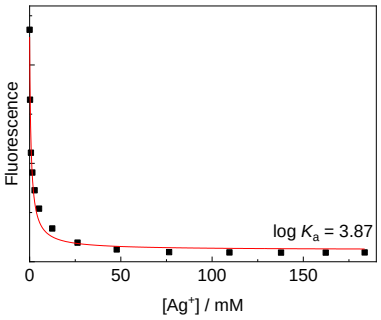
Fluorescence
log K_a = 3.87
0
50
100
150
[Ag^+] / mM

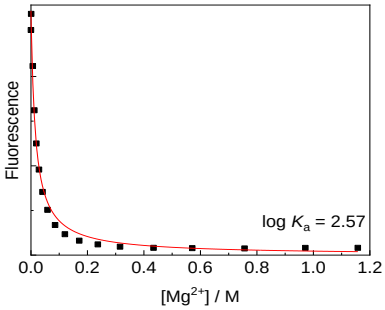
Fluorescence
log K_a = 2.57
0.0
0.2
0.4
0.6
0.8
1.0
1.2
[Mg^{2+}] / M

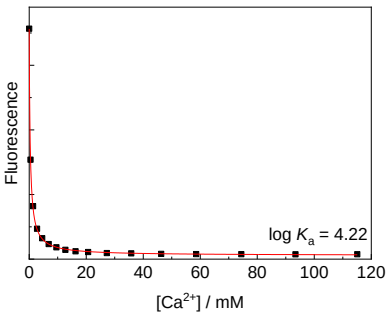
Fluorescence
log K_a = 4.22
0
20
40
60
80
100
120
[Ca^{2+}] / mM

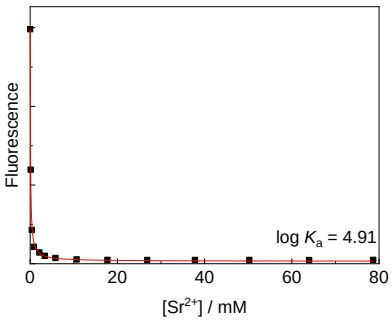
Fluorescence
log K_a = 4.91
0
20
40
60
80
[Sr^{2+}] / mM

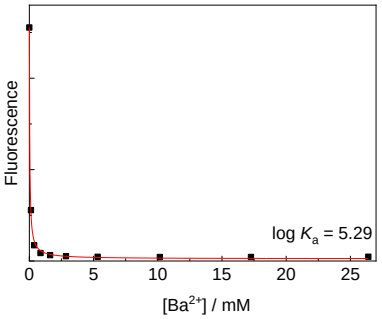
Fluorescence
log K_a = 5.29
0
5
10
15
20
25
[Ba^{2+}] / mM

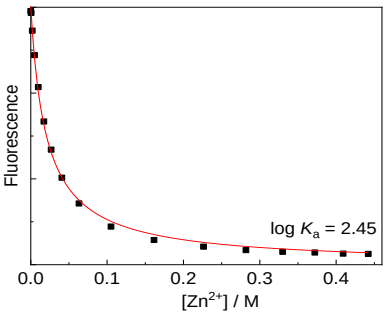
Fluorescence
log K_a = 2.45
0.0
0.1
0.2
0.3
0.4
[Zn^{2+}] / M

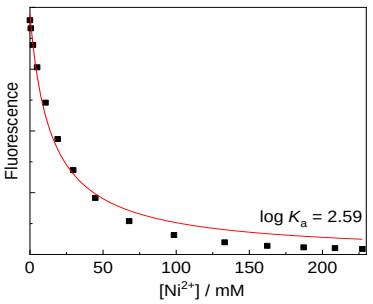
Fluorescence
log K_a = 2.59
0
50
100
150
200
[Ni^{2+}] / mM

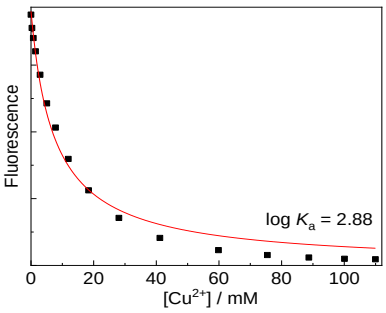
Fluorescence
log K_a = 2.88
0
20
40
60
80
100
[Cu^{2+}] / mM

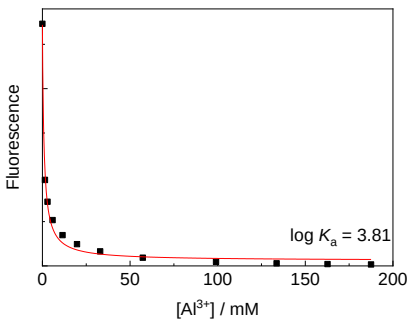
Fluorescence
log K_a = 3.81
0
50
100
150
200
[Al^{3+}] / mM

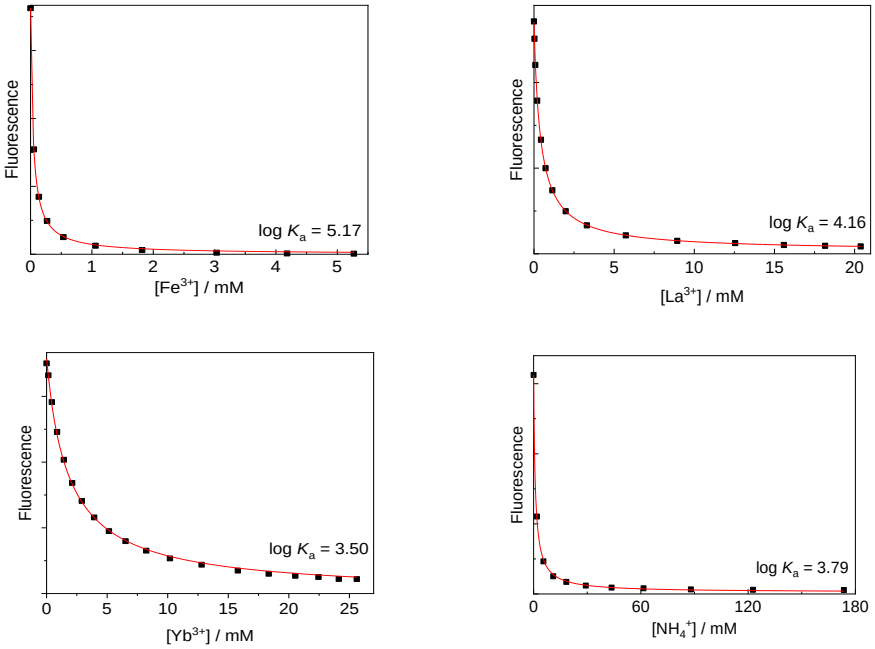

6.4. Competitive Displacement Experiments with CB7/BE and Cations

6.4.1. Determination of Binding Constant between CB7 and BE

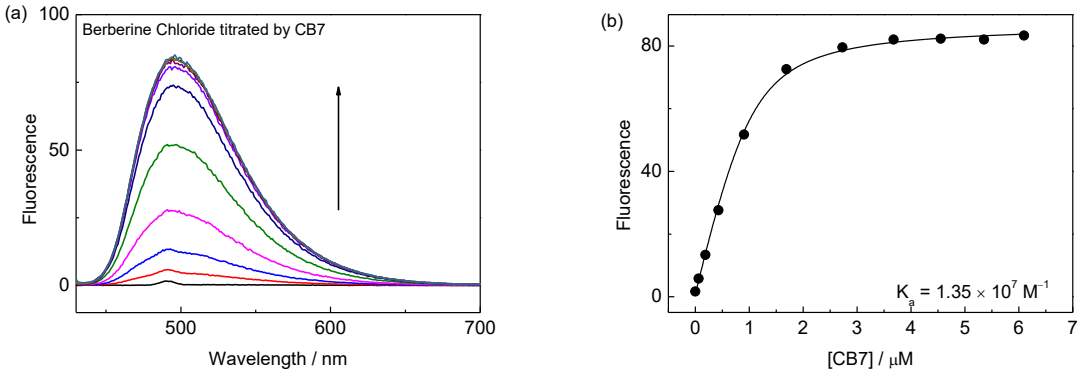

Figure S32: (a) Emission spectra of 1 μM BE, in aqueous solution, upon addition of CB7, λ_{ex} = 420 nm; (b) Plot of the emission intensity at 490 nm of 1 μM BE, in aqueous solution, versus concentration of CB7.

6.4.2. Representative Displacement Titration of CB7/BE with K^+

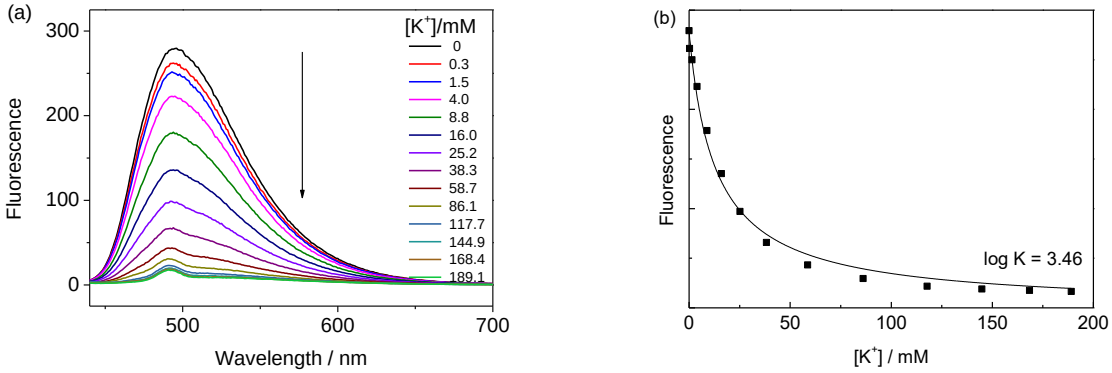

Figure S33: (a) Emission spectra of 3 μM BE and 0.5 μM CB7 in aqueous solution, upon addition of KCl, λ_{ex} = 420 nm; (b) Fitting plot of the emission intensity at 490 nm of BE versus concentration of KCl.

6.4.3. Normalized Emission Intensity of CB7/BE *versus* Cation Concentration

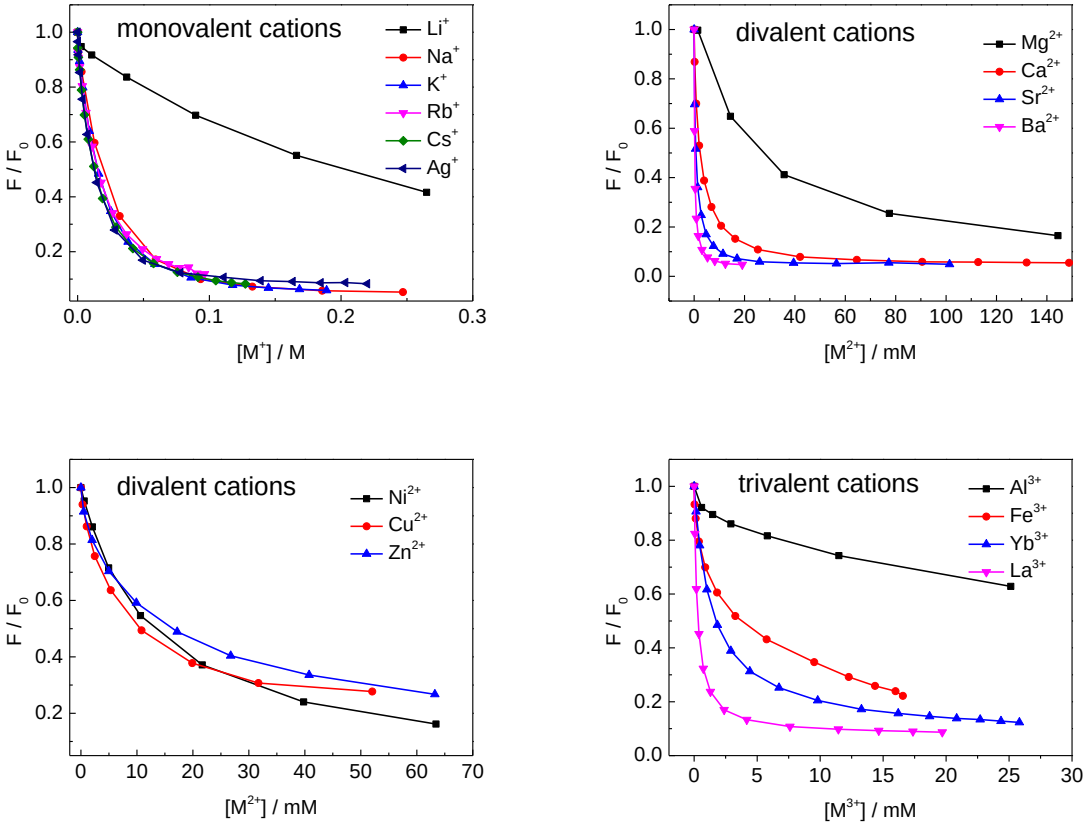

Figure S34: Plot of the normalized emission intensity at 490 nm of 3 μM BE and 0.5 μM CB7 versus concentrations of 17 different metal cations. (Data points connected by lines, not fitted.)

6.4.4. Comparison of ITC and Fluorescence-based Titrations

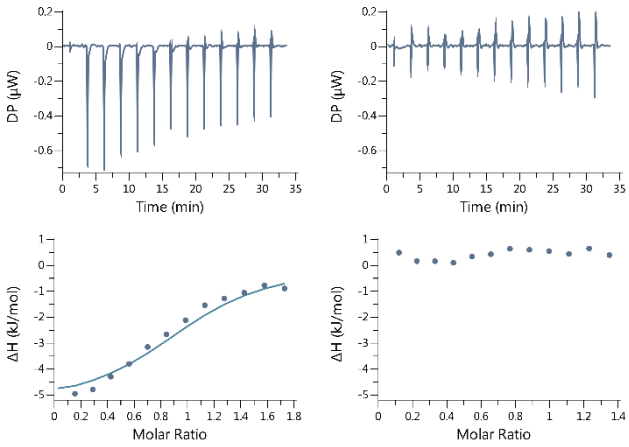

Figure S35: ITC isotherm for the titration of $La(NO_3)_3$ (c = 350 µM) into an aqueous CB7 solution (left, 39.0 µM) and in water (right, used for point-to-point correction) at 10 °C.

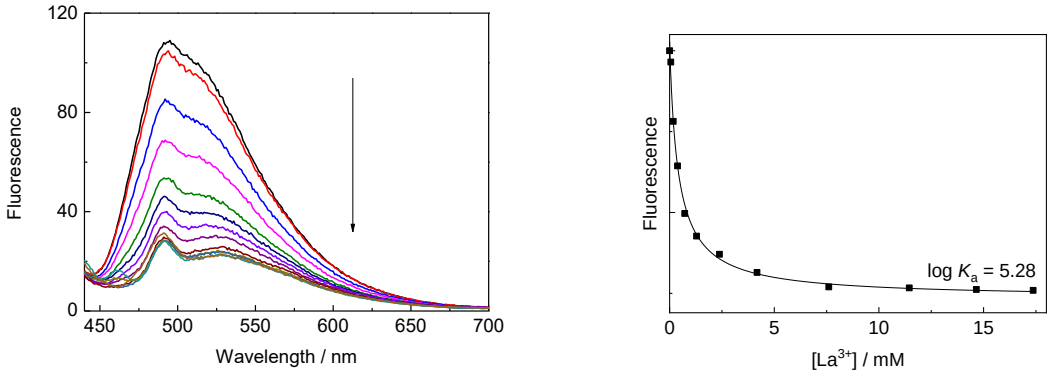

Figure S36: (a) Emission spectra of 3 µM BE and 0.5 µM CB7 in aqueous solution at 10 °C, upon addition of $LaCl_3$, λ_{ex} = 420 nm; (b) Fitting plot of the emission intensity at 490 nm of BE versus concentration of $LaCl_3$.

Table S8: Comparison of the binding constants determined by fluorescence spectroscopy and ITC of the complexation of La^{3+} (c = 350 µM) by CB7 (c = 39.0 µM) in water at 10 °C.

	K_a /·10^3 M^{-1}	log K_a
Fluorescence spectroscopy (BE)	190	5.28
ITC (10 °C)	180	5.25

6.4.5. Fitting Curves of Displacement Titrations between CB7/BE and Cations

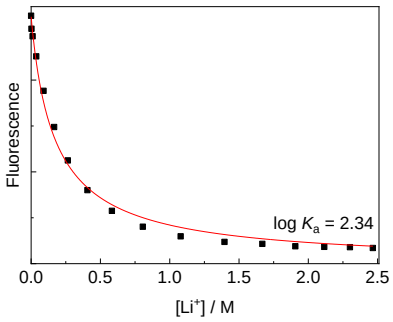

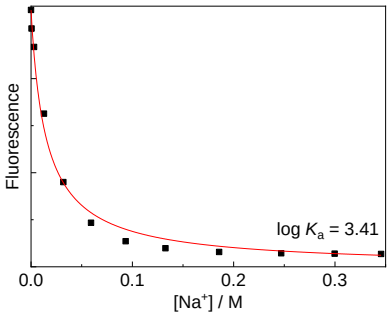

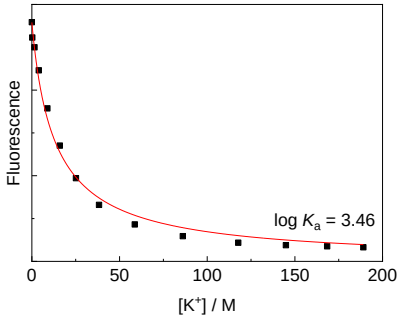

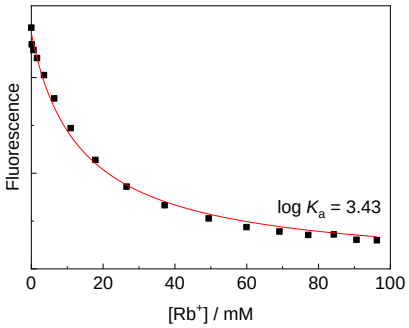

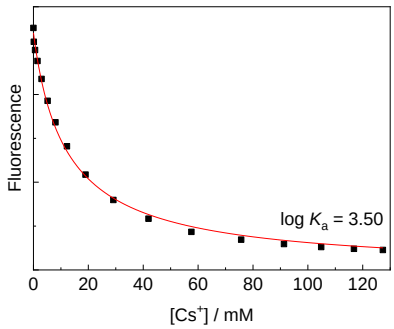

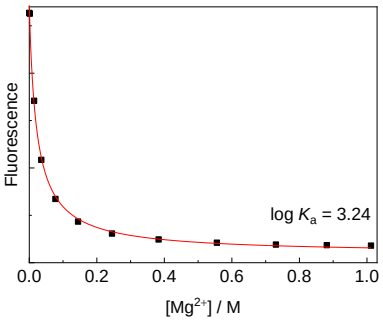

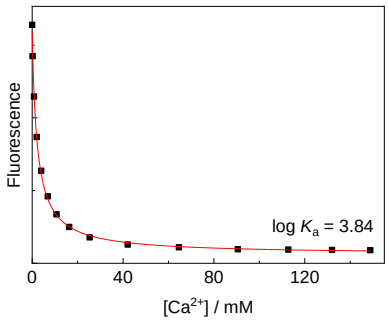

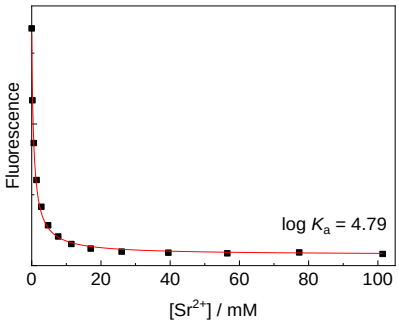

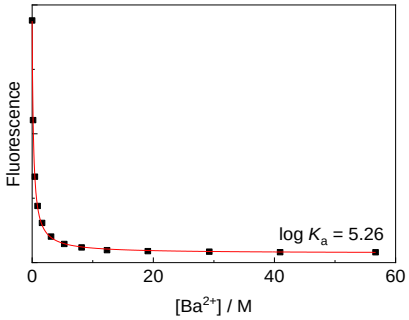
Fluorescence
log K_a = 5.26
0
20
40
60
[Ba^{2+}] / M

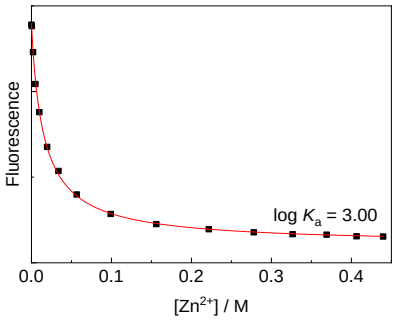
Fluorescence
log K_a = 3.00
0.0
0.1
0.2
0.3
0.4
[Zn^{2+}] / M

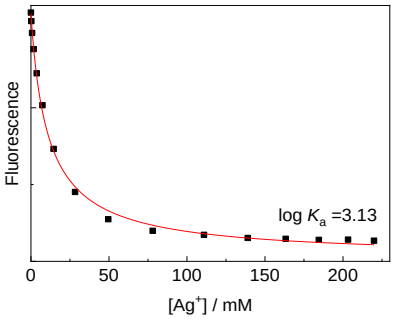
Fluorescence
log K_a =3.13
0
50
100
150
200
[Ag^{+}] / mM

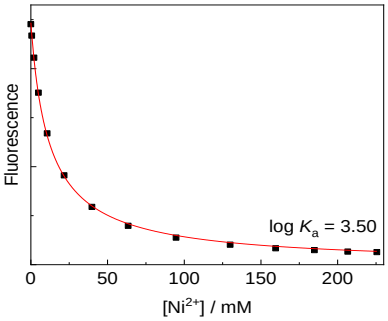
Fluorescence
log K_a = 3.50
0
50
100
150
200
[Ni^{2+}] / mM

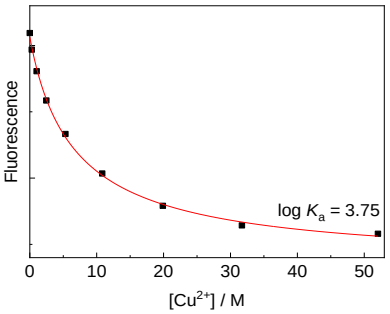
Fluorescence
log K_a = 3.75
0
10
20
30
40
50
[Cu^{2+}] / M

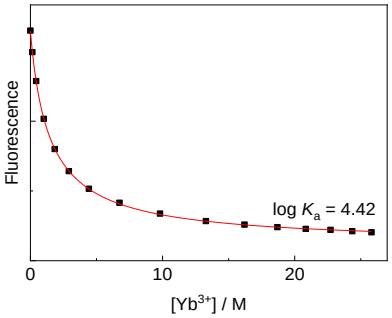
Fluorescence
log K_a = 4.42
0
10
20
[Yb^{3+}] / M

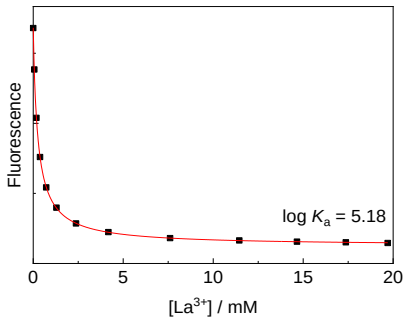
Fluorescence
log K_a = 5.18
0
5
10
15
20
[La^{3+}] / mM

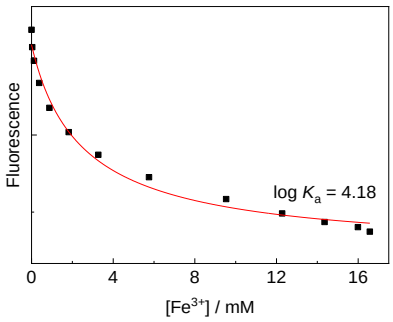
Fluorescence
log K_a = 4.18
0
4
8
12
16
[Fe^{3+}] / mM

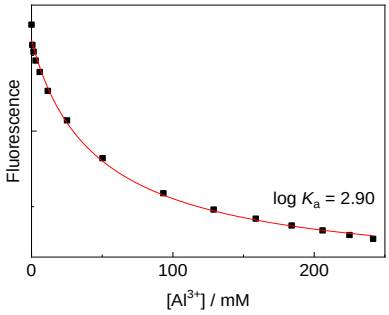
Fluorescence
log K_a = 2.90
0
100
200
[Al^{3+}] / mM

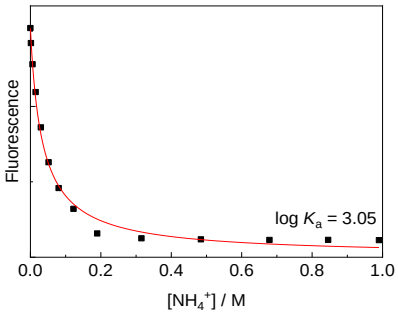
Fluorescence
log K_a = 3.05
0.0
0.2
0.4
0.6
0.8
1.0
[NH_4^+] / M

6.5. Competitive Displacement Experiments with CB8/PDI and Cations

6.5.1. Representative Displacement Titration of CB8/PDI with K^+

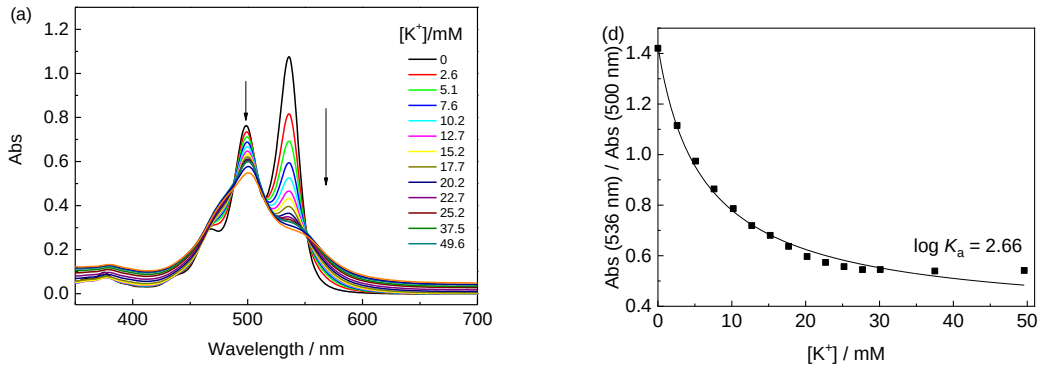

Figure S37: (a) Absorption spectra of 15 µM PDI and 15 µM CB8 in aqueous solution, upon addition of KCl; (b) Fitting plot of Abs (536 nm)/Abs (500 nm) of 15 µM PDI and 15 µM CB8 versus concentration of KCl.

6.5.2. Absorbance of CB8/PDI versus Cation Concentration

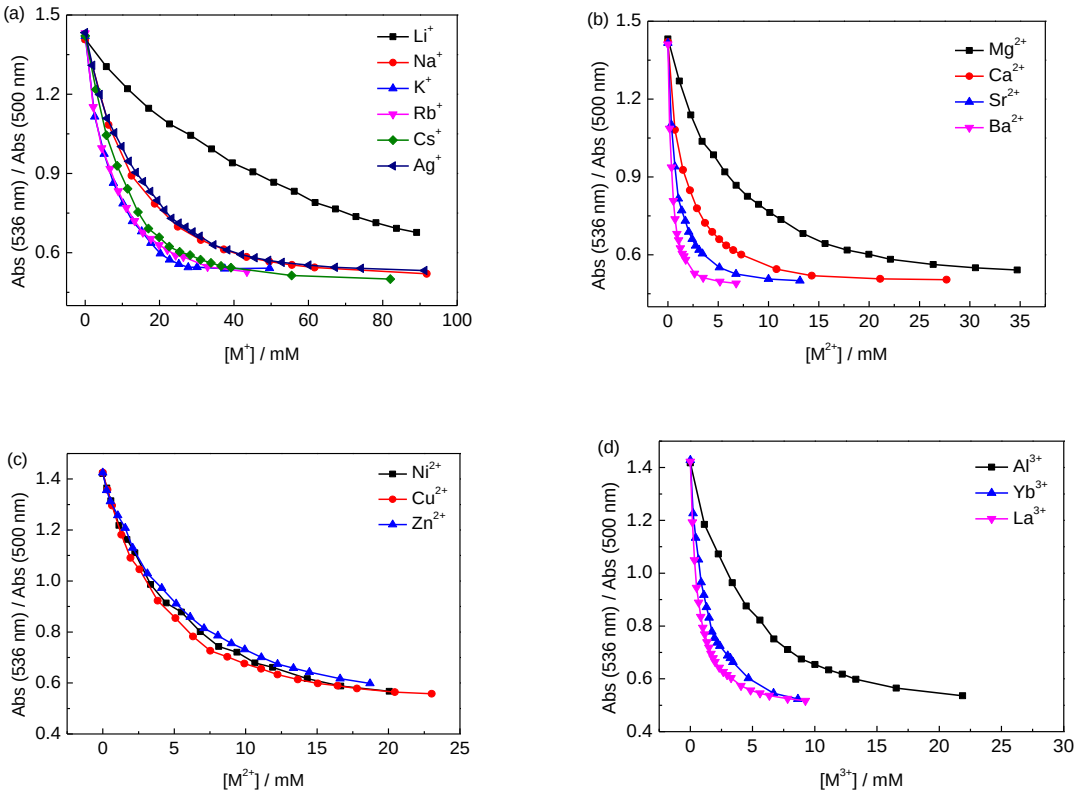

Figure S38: Plot of Abs (536 nm)/Abs (500 nm) of 15 µM PDI and 15 µM CB8 versus concentrations of 16 cations (Data points connected by lines, not fitted.)

6.5.3. Fitting Curves of Displacement Titrations between CB8/PDI and Cations

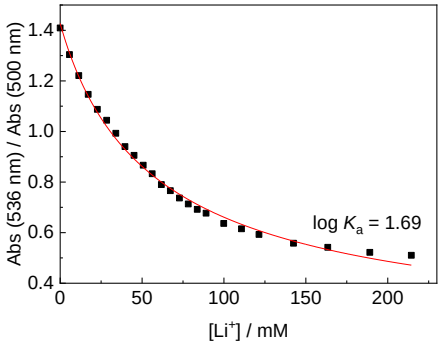

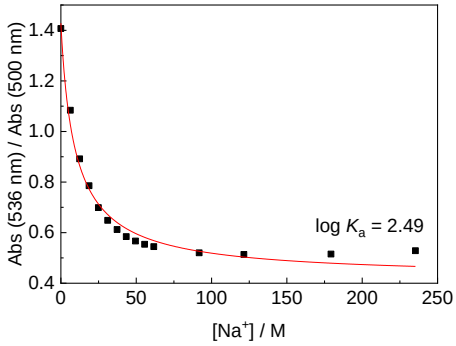

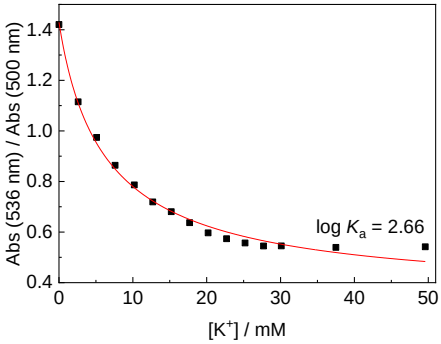

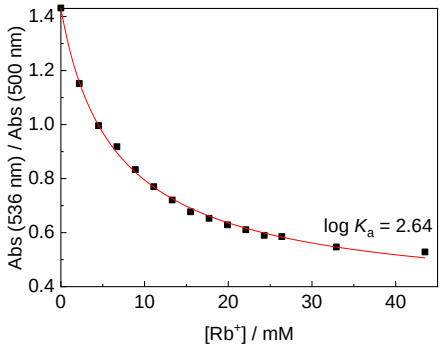

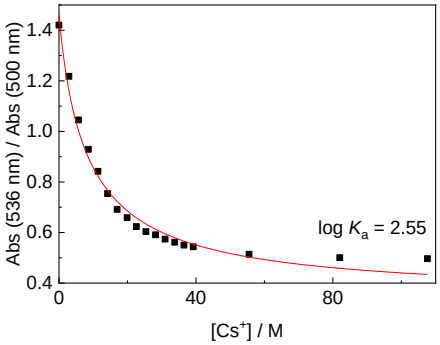

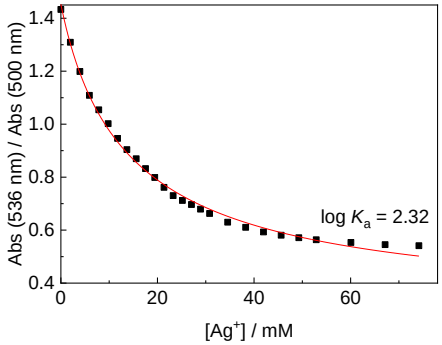

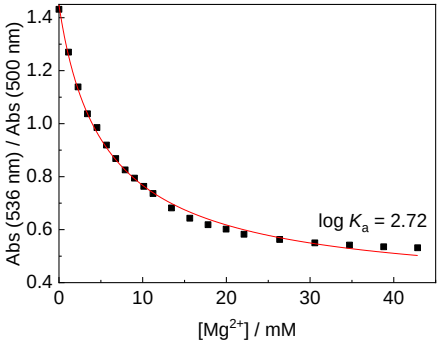

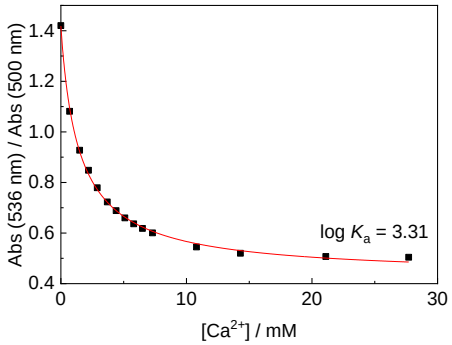

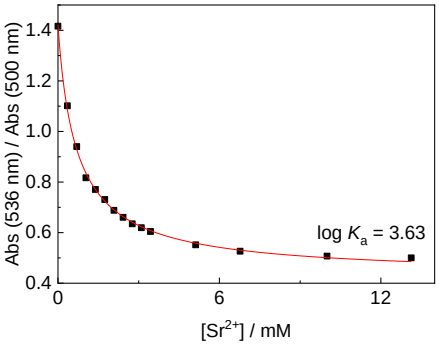
Abs (536 nm) / Abs (500 nm)
1.4
1.2
1.0
0.8
0.6
0.4
0
6
12
log K_a = 3.63
[Sr^{2+}] / mM

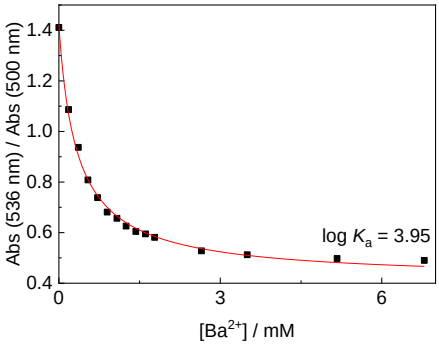
Abs (536 nm) / Abs (500 nm)
1.4
1.2
1.0
0.8
0.6
0.4
0
3
6
log K_a = 3.95
[Ba^{2+}] / mM

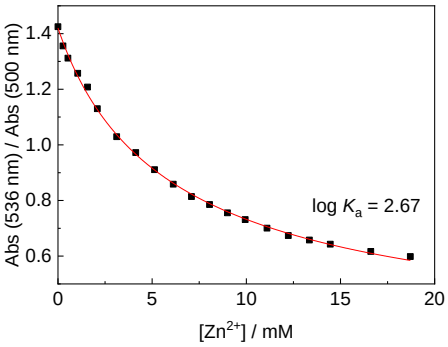
Abs (536 nm) / Abs (500 nm)
1.4
1.2
1.0
0.8
0.6
0
5
10
15
20
log K_a = 2.67
[Zn^{2+}] / mM

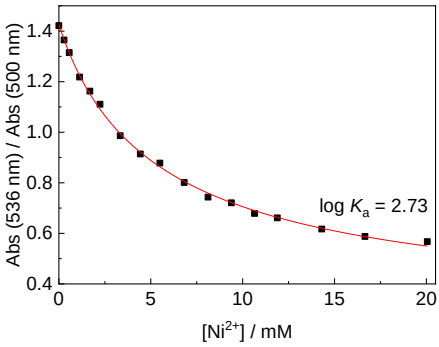
Abs (536 nm) / Abs (500 nm)
1.4
1.2
1.0
0.8
0.6
0.4
0
5
10
15
20
log K_a = 2.73
[Ni^{2+}] / mM

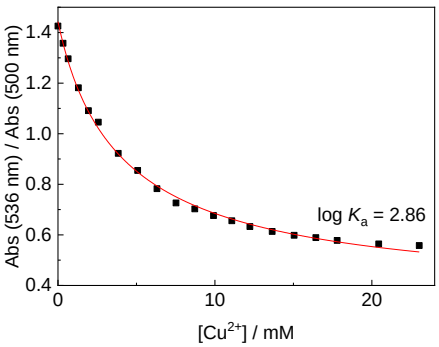
Abs (536 nm) / Abs (500 nm)
1.4
1.2
1.0
0.8
0.6
0.4
0
10
20
log K_a = 2.86
[Cu^{2+}] / mM

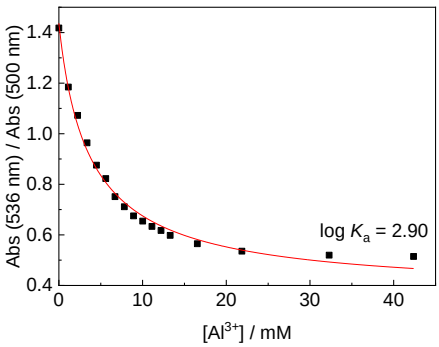
Abs (536 nm) / Abs (500 nm)
1.4
1.2
1.0
0.8
0.6
0.4
0
10
20
30
40
log K_a = 2.90
[Al^{3+}] / mM

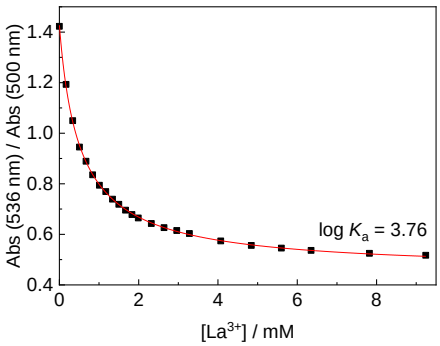
Abs (536 nm) / Abs (500 nm)
1.4
1.2
1.0
0.8
0.6
0.4
0
2
4
6
8
log K_a = 3.76
[La^{3+}] / mM

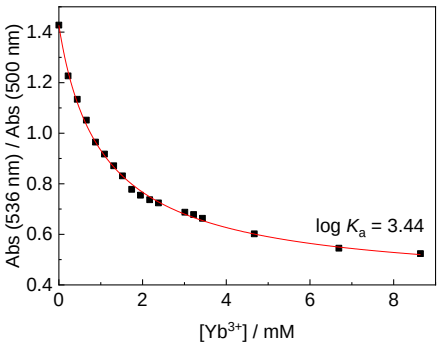
Abs (536 nm) / Abs (500 nm)
1.4
1.2
1.0
0.8
0.6
0.4
0
2
4
6
8
log K_a = 3.44
[Yb^{3+}] / mM

7. Supporting References

1. W. L. Mock and N. Y. Shih, *J. Org. Chem.*, 1986, **51**, 4440-4446.
2. H.-J. Buschmann, E. Cleve and E. Schollmeyer, *Anal. Chim. Acta*, 1992, **193**, 93-97.
3. R. Hoffmann, W. Knoche, C. Fenn and H.-J. Buschmann, *J. Chem. Soc. Faraday Trans.*, 1994, **90**, 1507-1511.
4. H.-J. Buschmann, K. Jansen, C. Meschke and E. Schollmeyer, *J. Solution Chem.*, 1998, **27**, 135-140.
5. H.-J. Buschmann, E. Cleve, K. Jansen, A. Wego and E. Schollmeyer, *J. Incl. Phenom. Macrocycl. Chem.*, 2001, **40**, 117-120.
6. H.-J. Buschmann, E. Cleve, K. Jansen and E. Schollmeyer, *Anal. Chim. Acta*, 2001, **437**, 157-163.
7. H.-J. Buschmann, K. Jansen and E. Schollmeyer, *Inorg. Chem. Commun.*, 2003, **6**, 531-534.
8. V. F. Pais, E. F. Carvalho, J. P. Tomé and U. Pischel, *Supramol. Chem.*, 2014, **26**, 642-647.
9. I. Hwang, W. S. Jeon, H. J. Kim, D. Kim, H. Kim, N. Selvapalam, N. Fujita, S. Shinkai and K. Kim, *Angew. Chem. Int. Ed.*, 2007, **46**, 210-213.
10. S. S. Thomas, H. Tang and C. Bohne, *J. Am. Chem. Soc.*, 2019, **141**, 9645-9654.
11. S. D. Choudhury, J. Mohanty, H. Pal and A. C. Bhasikuttan, *J. Am. Chem. Soc.*, 2010, **132**, 1395-1401.
12. S. He, F. Biedermann, N. Vankova, L. Zhechkov, T. Heine, R. E. Hoffman, A. De Simone, T. T. Duignan and W. M. Nau, *Nat. Chem.*, 2018, **10**, 1252-1257.
13. A. L. Koner, C. Márquez, M. H. Dickman and W. M. Nau, *Angew. Chem. Int. Ed.*, 2011, **50**, 545-548.
14. M. V. Rekharsky, Y. H. Ko, N. Selvapalam, K. Kim and Y. Inoue, *Supramol. Chem.*, 2007, **19**, 39-46.
15. Z. Li, S. Sun, F. Liu, Y. Pang, J. Fan, F. Song and X. Peng, *Dyes Pigm.*, 2012, **93**, 1401-1407.
16. G. Ghale and W. M. Nau, *Acc. Chem. Res.*, 2014, **47**, 2150-2159.
17. Z. Miskolczy and L. Biczók, *J. Phys. Chem. B*, 2014, **118**, 2499-2505.
18. F. Biedermann, E. Elmalem, I. Ghosh, W. M. Nau and O. A. Scherman, *Angew. Chem. Int. Ed.*, 2012, **124**, 7859-7863.
19. A. I. Lazar, F. Biedermann, K. R. Mustafina, K. I. Assaf, A. Hennig and W. M. Nau, *J. Am. Chem. Soc.*, 2016, **138**, 13022-13029.
20. H. Bakirci, A. L. Koner, T. Schwarzlose and W. M. Nau, *Chem. Eur. J.*, 2006, **12**, 4799-4807.
21. A. Bagno and G. Scorrano, *J. Am. Chem. Soc.*, 1988, **110**, 4577-4582.
22. I. Hwang, Woo S. Jeon, H.-J. Kim, D. Kim, H. Kim, N. Selvapalam, N. Fujita, S. Shinkai and K. Kim, *Angew. Chem. Int. Ed.*, 2007, **46**, 210-213.
23. R. M. Izatt, J. S. Bradshaw, S. A. Nielsen, J. D. Lamb, J. J. Christensen and D. Sen, *Chem. Rev.*, 1985, **85**, 271-339.
24. M. S. Díaz, M. L. Freile and M. I. Gutiérrez, *Photoch. Photobio. Sci.*, 2009, **8**, 970-974.
25. J. J. Jankowski, D. J. Kieber and K. Mopper, *Photochem. Photobiol.*, 1999, **70**, 319-328.
26. E. E. Sager and F. C. Byers, *J. Res. Natl. Bur. Stand.*, 1957, **57**.